Tunable Adaptive Target Detection With Kernels in Colocated MIMO Radar

Amir Zaimbashi, *Member, IEEE*, and Jian Li, *Member IEEE, Fellow IEEE*

***Abstract*—We introduce a framework for exploring adaptive target detection in colocated MIMO radar in non-linear feature space by exploiting the theory of kernel. The kernel theory inspires us to replace the inner products of test statistics with that of nonlinear mapped data in the feature space or that of their kernel tricks to achieve better detection performance. We apply this framework to the problem of tunable adaptive target detection in colocated MIMO radar, according to the principle of the generalized likelihood ratio (GLR), Rao and Wald (RaW) tests, and propose several new detectors under two new tunable detector forms, namely kernel tunable GLR-based and kernel tunable Raw-based detectors. The proposed tunable detectors include most of the prior detectors in colocated MIMO radar as special cases. One capability of the proposed detectors is that their robustness or selectivity (RoS) to steering vector mismatch (SVM) can be tuned flexibility through an RoS tuning parameter. In addition, we are able to incorporate the prior distribution (PD) of the disturbance covariance matrix, if available, through a PD tuning parameter. Therefore, the proposed detectors can be tuned based on the tuning RoS parameter to achieve robust or selective performance in the presence of SVM as well as to switch between the Bayesian or non-Bayesian based detectors through the PD parameter. For practical situations, we show that the proposed detectors possess CFAR property against disturbance covariance matrix by resorting to the invariance principle. Extensive Monte Carlo simulation results are provided to indicate that the proposed detectors have better detection performance than their counterparts in both single-target and multi-target scenarios.**

***Index Terms*—MIMO radar, detection theory, kernel theory, GLR test, Rao test, Wald test, Classical and Bayesian frameworks, Tunable detector, CFAR property.**

I. Introduction

DETECTION theory and estimation theory are essential to the design of digital signal processing receivers of communication systems for decision making and information extraction, respectively [1]. In particular, in detection theory, we encounter three different problems of the so-called signal activity detection (SAD), demodulation and classification (or pattern recognition). In all these problems, we need to decide among two or more possible hypotheses based on an observed data set [2]. Thus, the central problem addressed in the detection theory is to form a function of the observed data set, namely test statistic, and then make a decision based on the obtained test statistic and an appropriate detection threshold. Among them, the SAD is the simplest detection problem, where we aim to decide whether a specific signal is present or if only an interference signal (e.g., noise, clutter, and interfering targets) is present. Such statistical problem is referred to as the binary hypothesis testing problem since we wish to use the observed data as efficiently as possible in making a decision between two possible hypotheses. As such, there are various detection problems in digital communication systems, radar, sonar, image processing, which can usually be cast as the SAD problems [3]–[19].

In radar terminology, the SAD problem is known as target detection, which is a primary task in any radar system. Among the works of literature, the problem of radar target-detection in the presence of mismatched signals is an important topic, addressed in [20]–[25] by designing some tunable receivers. In this paper, we focus on target detection through colocated multiple-input multiple-output (C-MIMO) radar, which makes it possible to estimate targets' parameters as well as to detect targets without requiring any training data and pulse compression [26]. In this context, abundant literatures exist on the C-MIMO target detection; see [27]–[32] and references therein. In these works, some tunable detectors in classical and Bayesian frameworks have been derived according to the generalized-likelihood ratio (GLR), Rao and Wald principles, where it was assumed that no training data is available.

Kernel-based approaches have offered great performance in real-world nonlinear decision problems by developing nonlinear algorithms in which the nonlinear characteristics of input data are exploited through the use of nonlinear kernel functions [33]. Kernel functions are similarity measures that implicitly exploit the structural information of input data by mapping them to a higher dimensional space, known as feature space [34]. In the context of SAD problems, there are few works exploiting the benefit of the kernel theory to discriminate between two possible hypotheses aimed at obtaining more efficient decision methods [35]–[38]. For example, an improved fault detection algorithm to enhance monitoring abilities of nonlinear biological processes was proposed in [35], relying on generalized likelihood ratio test (GLRT) and kernel-based principal component analysis (KPCA). It was shown that the kernel-based GLRT improved the fault detection capability, however, the detection performance was not investigated in terms of the detection theory metrics, particularly detection probability curves and false alarm

Manuscript received November 5, 2019; revised January 21, 2020 and February 13, 2020; accepted February 14, 2020. Date of publication February 21, 2020; date of current version March 11, 2020. The associate editor coordinating the review of this manuscript and approving it for publication was Prof. C. Murthy. This work was supported by the NSF under Grant 1708509. *(Corresponding author: Amir Zaimbashi.)*

Amir Zaimbashi is with the Optical and RF Communication Systems (ORCS) Laboratory, Department of Electrical Engineering, Shahid Bahonar University of Kerman, Kerman 76169-14111, Iran (e-mail: a.zaimbashi@uk.ac.ir).

Jian Li is with the Department of Electrical and Computer Engineering, University of Florida, Gainesville, FL 32611 USA (e-mail: li@dsp.ufl.edu).

Digital Object Identifier 10.1109/TSP.2020.2975371

behavior. A kernel-based matched subspace detector (K-MSD) for subpixel target detection in hyperspectral imagery was, in turn, proposed in [36]. It was shown that the K-MSD obtained superior detection performance compared to the conventional MSD. In [37], an accurate kernelized energy detection approach in Gaussian and non-Gaussian noise scenarios was developed for spectrum sensing purposes. In [38], the KMSD algorithm was adopted for spectrum sensing tasks in a cognitive radio system to improve the detection performance of the conventional MSD in low signal-to-noise ratio (SNR) regimes.

However, all these aforementioned kernel-based detectors have been proposed for real-valued measurements. For the first time, in this paper, we aim to combine the idea of kernel theory and detection theory to develop new target detection algorithms for C-MIMO radars, working with complex-valued baseband measurements. To illustrate this, we consider the target-detection problem in C-MIMO radar introduced in [29]–[32], where the authors proposed different algorithms based on the GLR, Rao and Wald principles as well as Bayesian GLR (BGLR), Bayesian Rao (BRao), Bayesian Wald (BWald) tests in the original input space. We firstly unify them and propose a new detector, then eight kernel-based detectors corresponding to the above detectors according to the polynomial kernel function are proposed, resulting overall in nine new detectors. The principle of invariance is exploited to examine the potential CFAR behavior of the proposed classical detectors against the disturbance covariance matrix. The so-obtained analytical results show that the proposed classical detectors possess CFAR behavior against the disturbance covariance matrix. We provide extensive simulation results to show that the proposed detectors significantly outperform their counterparts.

The rest of this paper is organized as follows: in Section II, the target detection problem via C-MIMO radar is formulated as a composite hypothesis testing problem. In Section III, the previously proposed detectors are unified according to simple similarity measure, namely inner product. Besides, a new detector is proposed. In Section IV, firstly, some preliminaries about kernel theory are introduced. Then, we propose eight new approaches for C-MIMO target detection scenarios. The CFAR property of the proposed classical detectors is examined in Section V. Extensive simulations result are given in Section VI, and Section VII concludes this article.

Notations: The superscripts $(.)^T$, $(.)^*$, and $(.)^\dagger$ denote the transpose, complex conjugate and the Hermitian (conjugate transpose), respectively. All vectors and matrices are denoted by bold lower case and bold upper case letters, respectively. $\mathbf{I}$ is the identity matrix. $\mathbf{0}$ represents the all-zero matrix. $||\mathbf{b}||$ denotes the Euclidean norm of vector $\mathbf{b}$, $|\alpha|$ represents the absolute value of scaler α, and $\langle \mathbf{a}, \mathbf{g} \rangle$ represents the inner product between vectors $\mathbf{a}$ and $\mathbf{g}$, defined as $\mathbf{a}^\dagger \mathbf{g}$ for complex domains. Finally, the imaginary unit is defined as $j = \sqrt{-1}$.

II. Problem Formulation

As in Fig. 1, consider a monostatic MIMO radar system consisting of two colocated uniform linear arrays (ULAs) of M transmit antennas and N receive antennas, where without loss of generality we assume that $M = N$. Let the antenna spacing be d and all transmit antennas operate at the same carrier frequency f_c, corresponding to carrier wavelength of $\lambda = \frac{c}{f_c}$ with c being the light speed. Let $\mathbf{s}(t) = [s_1(t), \ldots, s_M(t)]^T$ be the complex baseband transmit signal vector emitted from the M transmit antennas, where $s_m(t)$ represents the equivalent baseband transmitted waveform from the m-th transmit antenna. For a constant radial velocity and point-like target located in the far-field at direction θ_1 and under spatial-narrowband effect, the received signal vector through the different receive antennas can be written as [30]

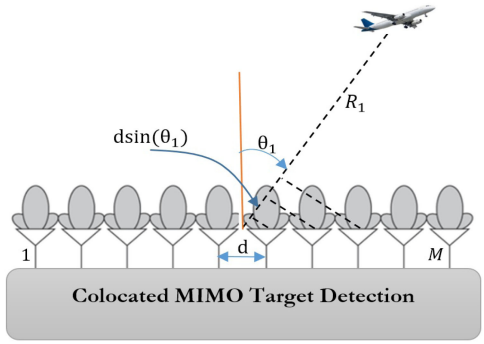

Fig. 1. Colocated MIMO radar target detection scenario.

$$\mathbf{y}'(t) = \alpha_1' e^{-j2\pi f_d^{(1)} t} \mathbf{a}_R(\theta_1) \mathbf{a}_T^\dagger(\theta_1) \mathbf{s}(t - \tau_1) + n(t), \quad (1)$$

where $0 \le t \le T_I$ with T_I being the integration time, $f_d^{(1)} = \frac{2v_r^{(1)}}{\lambda}$ with $v_r^{(1)}$ being the target velocity, and $\tau_1 = \frac{2R_1}{c}$ with R_1 being the one-way range between the target and a reference point, as shown in Fig. 1. Here, the complex value α_1' is the corresponding path loss, assumed to be identical for all transmit and receive antennas due to the far-field assumption. In (1), $\mathbf{a}_T$ and $\mathbf{a}_R$ are respectively transmit and receive steering vectors, given by

$$\mathbf{a}_T = \left[e^{j2\pi(\frac{M+1}{2}-1)\frac{d}{\lambda}\sin(\theta_1)}, \ldots, e^{j2\pi(\frac{M+1}{2}-M)\frac{d}{\lambda}\sin(\theta_1)} \right]^T \quad (2)$$

$$\mathbf{a}_R = \left[e^{-j2\pi(\frac{M+1}{2}-1)\frac{d}{\lambda}\sin(\theta_1)}, \ldots, e^{-j2\pi(\frac{M+1}{2}-M)\frac{d}{\lambda}\sin(\theta_1)} \right]^T \quad (3)$$

Consider that the transmitted signal is a sequence of K modulated baseband pulses $\mathbf{p}_k(t)$ with an equal width of τ, for $k = 0, \ldots, K-1$, with a constant pulse repetition interval (PRI) of T_P, i.e.,

$$\mathbf{s}(t) = \sum_{k=0}^{K} \mathbf{p}_k(t - kT_P) \quad (4)$$

Then, (1) can be written as

$$\mathbf{y}'(t) = \alpha_1 \mathbf{a}_R \mathbf{a}_T^\dagger \sum_{k=0}^{K} e^{-j2\pi f_d^{(1)} kT_P} \mathbf{p}_k(t - kT_P - \tau_1) + n(t) \quad (5)$$

where $\alpha_1 = \alpha_1' e^{-j2\pi f_d^{(1)}\tau_1}$. Here, we assume that $f_d^{(1)}\tau << 1$ to arrive at $e^{j2\pi f_d^{(1)}t}\mathbf{p}_k(t - kT_P - \tau_1) \approx e^{j2\pi f_d^{(1)}\tau_1} e^{-j2\pi f_d^{(1)}kT_P}\mathbf{p}_k(t - kT_P - \tau_1)$. For a specific range-Doppler coordinate, after compensation, the received signal during the k-th pulse can be represented as

$$\mathbf{y}_k(t) = \alpha_1 \mathbf{a}_R \mathbf{a}_T^\dagger \mathbf{p}_k(t - kT_P) + n_k(t) \tag{6}$$

Let $\mathbf{P}_k$ be an $M \times Q$-dimensional matrix, standing for the discrete version of the spatial-temporal complex baseband transmitted signal through different transmit antennas and during the k-th pulse. Here, Q is the number of samples of each transmitted pulse, i.e., $Q = \tau f_s$ with f_s being the sampling frequency satisfying Nyquist sampling theorem. Thus, the discrete version of $\mathbf{y}_k(t)$ corresponding to the pulse width τ, denoted by $\mathbf{Y}_k$, can be written as

$$\mathbf{Y}_k = \alpha_1 \mathbf{a}_R \mathbf{a}_T^\dagger \mathbf{P}_k + \mathbf{N}_k \tag{7}$$

Define

$$\mathbf{Y} = [\mathbf{Y}_1, \ldots, \mathbf{Y}_K] \in C^{N \times QK}, \tag{8}$$

$$\mathbf{N} = [\mathbf{N}_1, \ldots, \mathbf{N}_K] \in C^{N \times QK}, \tag{9}$$

and

$$\mathbf{P} = [\mathbf{P}_1, \ldots, \mathbf{P}_K] \in C^{M \times QK} \tag{10}$$

Then, the received data during the integration time can be compactly represented as

$$\mathbf{Y} = \alpha_1 \mathbf{a}_R \mathbf{a}_T^\dagger \mathbf{P} + \mathbf{N} \tag{11}$$

where the target-detection problem can be modeled as a composite hypothesis testing problem, given by

$$\begin{cases} H_0 : \mathbf{Y} = \mathbf{N} \\ H_1 : \mathbf{Y} = \alpha_1 \mathbf{a}_R \mathbf{a}_T^\dagger \mathbf{P} + \mathbf{N}. \end{cases} \tag{12}$$

where

- The scalar α_1 is assumed to be a complex, unknown but deterministic parameter. It can be considered as a random variable according to Swerling 1 target model (i.e., α_1 is modeled as a complex Gaussian random variable), however, we focus on the deterministic unknown one here. In both cases, this implies that K echoes collected on one scan have the same value.
- In the case of the C-MIMO radar receiver with a symmetrically spaced linear array, the vector $\mathbf{a}_R$ is also persymmetric, satisfying $\mathbf{a}_R = \mathbf{J}\mathbf{a}_R^\dagger$. Here, both steering vectors $\mathbf{a}_R$ and $\mathbf{a}_T$ are assumed to be known.
- The columns of matrix $\mathbf{N}$ are assumed to be independent and identically distributed (IID), and have a circularly symmetric, complex Gaussian distribution with zero mean and unknown covariance matrix $\mathbf{R}$, i.e., $\mathbf{n}_l \sim \mathcal{CN}(\mathbf{0}, \mathbf{R})$ for $l = 1, \ldots, QK$. In the Bayesian framework, it is assumed that the covariance matrix $\mathbf{R}$ is unknown but stochastic with a specific prior density distribution. The inverse complex Wishart distribution is a widely adopted prior distribution for the covariance matrix $\mathbf{R}$ [32], i.e.,

$$\mathbf{R} \sim \mathcal{W}^{-1}(\gamma, \gamma \mathbf{R}_0) \tag{13}$$

where $\mathbf{R}_0$ is a known positive definite $N \times N$ matrix and can be considered as the prior information on the average covariance matrix, γ is the degree of freedom measuring the reliability of the prior information, where $\gamma \geq N$ [32]. In some literature, the persymmetric structure of the covariance matrix $\mathbf{R}$ is exploited to improve the target-detection performance [39]–[42]. More precisely, $\mathbf{R}$ has persymmetric structure, satisfying $\mathbf{R} = \mathbf{J}\mathbf{R}^\dagger\mathbf{J}$ where $N \times N$ matrix $\mathbf{J}$ is called the exchange matrix. In this article, we do not use these properties to devise our new detectors and they are left for another work.
- It is also assumed that no target-free training data are available due to many practical factors such as the presence of interfering targets and variations in terrain [43]–[45].

In (12), the hypothesis H_0 is referred to as the null hypothesis, and H_1 is known as the alternative hypothesis. Considering all this, we can now reformulate our composite hypothesis testing problem as

$$\begin{cases} H_0 : \alpha_1 = 0 \\ H_1 : \alpha_1 \neq 0. \end{cases} \tag{14}$$

This clearly shows that the unknown covariance matrix $\mathbf{R}$ is a nuisance parameter, i.e., it is not relevant to the decision. Thus, it is important to devise detectors having CFAR property against the disturbance covariance matrix $\mathbf{R}$.

TABLE I
PRIOR DETECTORS

Detector	Detector	Reference
Rao	$\frac{\lvert\mathbf{a}_r^\dagger(\mathbf{Y}\mathbf{Y}^\dagger)^{-1}\mathbf{Y}\mathbf{P}^\dagger\mathbf{a}_t\rvert^2}{\mathbf{a}_r^\dagger(\mathbf{Y}\mathbf{Y}^\dagger)^{-1}\mathbf{a}_r\mathbf{a}_t^\dagger\mathbf{P}\mathbf{P}^\dagger\mathbf{a}_t} \underset{H_0}{\overset{H_1}{\gtrless}} \eta_1'$	[30]
Wald	$\frac{\lvert\mathbf{a}_r^\dagger(\mathbf{Y}\mathbf{D}^\perp\mathbf{Y}^\dagger)^{-1}\mathbf{Y}\mathbf{P}^\dagger\mathbf{a}_t\rvert^2}{\mathbf{a}_r^\dagger(\mathbf{Y}\mathbf{D}^\perp\mathbf{Y}^\dagger)^{-1}\mathbf{a}_r\mathbf{a}_t^\dagger\mathbf{P}\mathbf{P}^\dagger\mathbf{a}_t} \underset{H_0}{\overset{H_1}{\gtrless}} \eta_2'$	[30]
TuRW	$\frac{\lvert\mathbf{a}_r^\dagger(\mathbf{Y}\mathbf{D}^\perp\mathbf{Y}^\dagger+\beta\mathbf{Y}\mathbf{D}\mathbf{Y}^\dagger)^{-1}\mathbf{Y}\mathbf{P}^\dagger\mathbf{a}_t\rvert^2}{\mathbf{a}_r^\dagger(\mathbf{Y}\mathbf{D}^\perp\mathbf{Y}^\dagger+\beta\mathbf{Y}\mathbf{D}\mathbf{Y}^\dagger)^{-1}\mathbf{a}_r\mathbf{a}_t^\dagger\mathbf{P}\mathbf{P}^\dagger\mathbf{a}_t} \underset{H_0}{\overset{H_1}{\gtrless}} \eta_3'$	[31]
BRao	$\frac{\lvert\mathbf{a}_r^\dagger(\mathbf{Y}\mathbf{Y}^\dagger+\gamma\mathbf{C})^{-1}\mathbf{Y}\mathbf{P}^\dagger\mathbf{a}_t\rvert^2}{\mathbf{a}_r^\dagger(\mathbf{Y}\mathbf{Y}^\dagger+\gamma\mathbf{C})^{-1}\mathbf{a}_r\mathbf{a}_t^\dagger\mathbf{P}\mathbf{P}^\dagger\mathbf{a}_t} \underset{H_0}{\overset{H_1}{\gtrless}} \eta_4'$	[32]
BWald	$\frac{\lvert\mathbf{a}_r^\dagger(\mathbf{Y}\mathbf{D}^\perp\mathbf{Y}^\dagger+\gamma\mathbf{C})^{-1}\mathbf{Y}\mathbf{P}^\dagger\mathbf{a}_t\rvert^2}{\mathbf{a}_r^\dagger(\mathbf{Y}\mathbf{D}^\perp\mathbf{Y}^\dagger+\gamma\mathbf{C})^{-1}\mathbf{a}_r\mathbf{a}_t^\dagger\mathbf{P}\mathbf{P}^\dagger\mathbf{a}_t} \underset{H_0}{\overset{H_1}{\gtrless}} \eta_5'$	[32]
BTuRW	$\frac{\lvert\mathbf{a}_r^\dagger(\mathbf{Y}\mathbf{D}^\perp\mathbf{Y}^\dagger+\beta\mathbf{Y}\mathbf{D}\mathbf{Y}^\dagger+\gamma\mathbf{C})^{-1}\mathbf{Y}\mathbf{P}^\dagger\mathbf{a}_t\rvert^2}{\mathbf{a}_r^\dagger(\mathbf{Y}\mathbf{D}^\perp\mathbf{Y}^\dagger+\beta\mathbf{Y}\mathbf{D}\mathbf{Y}^\dagger+\gamma\mathbf{C})^{-1}\mathbf{a}_r\mathbf{a}_t^\dagger\mathbf{P}\mathbf{P}^\dagger\mathbf{a}_t} \underset{H_0}{\overset{H_1}{\gtrless}} \eta_6'$	This paper
GLR	$\frac{\mathbf{a}_r^\dagger(\mathbf{Y}\mathbf{D}^\perp\mathbf{Y}^\dagger)^{-1}\mathbf{a}_r}{\mathbf{a}_r^\dagger(\mathbf{Y}\mathbf{Y}^\dagger)^{-1}\mathbf{a}_r} \underset{H_0}{\overset{H_1}{\gtrless}} \eta_7'$	[29]
BGLR	$\frac{\mathbf{a}_r^\dagger(\mathbf{Y}\mathbf{D}^\perp\mathbf{Y}^\dagger+\gamma\mathbf{C})^{-1}\mathbf{a}_r}{\mathbf{a}_r^\dagger(\mathbf{Y}\mathbf{Y}^\dagger+\gamma\mathbf{C})^{-1}\mathbf{a}_r} \underset{H_0}{\overset{H_1}{\gtrless}} \eta_8'$	[32]

III. UNIFYING PREVIOUS ADAPTIVE DETECTORS

In this section, we first introduce seven prior methods including GLR, Rao, Wald, tunable Rao/Wald (TuRW), Bayesian GLR (BGLR), Bayesian Rao (BRao) and Bayesian Wald (BWald) detectors, for the detection problem (14). Next, we unify the Rao, Wald, TuRW, BRao, BWald, BTuRW, GLR and BGLR tests, listed in Table I, where the BTuRW detector is a new proposed detector in this paper. To this end, let us define the following

TABLE II
SPECIAL CASES OF THE GENERAL DETECTORS (22) AND (24)

Detector	Special Detectors	(β, κ)	Threshold
T-RaW(β, κ)	Rao	$(1, 0)$	η_1
	Wald	$(0, 0)$	η_2
	TuRW	$(\beta \geq 0, 0)$	η_3
	BRao	$(1, 1)$	η_4
	BWald	$(0, 1)$	η_5
	BTuRW	$(\beta \geq 0, 1)$	η_6
T-GLR(κ)	GLR	$(1, 0)$	η_7
	BGLR	$(1, 1)$	η_8

vectors and matrices so as to facilitate further discussion:

$$\mathbf{b} = \frac{\mathbf{P}^{\dagger}\mathbf{a}_T}{||\mathbf{P}^{\dagger}\mathbf{a}_T||}, \tag{15}$$

$$\mathbf{D} = \mathbf{b}\mathbf{b}^H, \tag{16}$$

$$\mathbf{D}^{\perp} = \mathbf{I} - \mathbf{b}\mathbf{b}^H, \tag{17}$$

$$\mathbf{R}(\beta, \kappa) = \mathbf{Y}\mathbf{D}^{\perp}\mathbf{Y}^{\dagger} + \beta\mathbf{Y}\mathbf{D}\mathbf{Y}^H + \kappa\gamma\mathbf{C} \tag{18}$$

$$\mathbf{Y}_w(\beta, \kappa) = \mathbf{R}^{-\frac{1}{2}}(\beta, \kappa)\mathbf{Y}, \tag{19}$$

$$\mathbf{a}(\beta, \kappa) = \frac{\mathbf{R}^{-\frac{1}{2}}(\beta, \kappa)\mathbf{a}_R}{||\mathbf{R}^{-\frac{1}{2}}(\beta, \kappa)\mathbf{a}_R||} \tag{20}$$

$$\mathbf{g}(\beta, \kappa) = \mathbf{Y}_w(\beta, \kappa)\mathbf{b} \tag{21}$$

Now, an alternative and unifying representations of the Rao, Wald, TuRW, BRao, BWald and BTuRW detectors can be written as

$$\Lambda_{\text{T-RaW}}(\mathbf{Y}; \beta, \kappa) = |\langle \mathbf{a}(\beta, \kappa), \mathbf{g}(\beta, \kappa)\rangle|^2 \underset{H_0}{\overset{H_1}{\gtrless}} \eta_i \tag{22}$$

where $\mathbf{g}$ can be considered as coherent integration along the column direction $\mathbf{b}$, performed by postmultiplying the whitened data $\mathbf{Y}_w$ with $\mathbf{b}$. In (22), $\langle \mathbf{a}, \mathbf{g}\rangle$ denotes the inner product of vectors $\mathbf{a}$ and $\mathbf{g}$, defined as $\mathbf{a}^{\dagger}\mathbf{g}$. In Table II, the special cases of the general proposed detector (22) is represented by particularizing the parameters β and κ. The decision thresholds η_i's are modification detection thresholds, depending on the tuning parameters β and κ, system parameters (i.e., M, N) and the desired false alarm rate, denoted by p_{fa}. This general and tunable (T) Rao and Wald -based detector is referred to as T-RaW(β, κ) in the sequel.

In [29] and [32], two adaptive detectors different from the Rao and Wald tests are devised according to the GLRT principle in the context of C-MIMO radar. One of them is based on the classical approach, while another is according to the Bayesian framework to achieve detection performance gains by incorporating prior knowledge about the disturbance covariance matrix. After some algebraic manipulations, we can unify them as follows

$$\frac{\mathbf{a}_r^H\mathbf{R}(0, \kappa)\mathbf{a}_r}{\mathbf{a}_r^H\mathbf{R}(1, \kappa)\mathbf{a}_r} \underset{H_0}{\overset{H_1}{\gtrless}} \eta'_{7+\kappa} \tag{23}$$

or, equivalently, as

$$\Lambda_{\text{T-GLR}}(\mathbf{Y}; \kappa) = \frac{|\langle \mathbf{a}(1, \kappa), \mathbf{g}(1, \kappa)\rangle|^2}{1 + \langle \mathbf{g}(1, \kappa), \mathbf{g}(1, \kappa)\rangle} \underset{H_0}{\overset{H_1}{\gtrless}} \eta_{7+\kappa} \tag{24}$$

It is interesting to note that the proposed unified detector (24) is quite general, including the GLR and BGLR detectors as special cases. More precisely, when $\kappa = 0$, the proposed detector corresponds to the GLR detector of [29], while it reduces to the BGLR test proposed in [32] for $\kappa = 1$. The special cases of the general GLR-based detector (24) are described by the parameter κ and their corresponding thresholds in Table II. In the following, this general and tunable GLR -based detector is referred to as T-GLR(κ).

IV. KERNEL-BASED ADAPTIVE DETECTORS

In this section, we first provide some preliminaries about kernel theory. Then the proposed kernel-based detectors will be introduced to offer much better detection performances as compared with the state-of-the-art detectors.

A. Preliminaries

In the unified detectors (22) and (24), the inner product $\langle \mathbf{a}, \mathbf{g}\rangle$ can provide a proper measure of similarity between vectors $\mathbf{a}$ and $\mathbf{g}$ if the representation space of the vectors $\mathbf{a}$ and $\mathbf{g}$ (i.e., original space) is rich enough. In many problems, the original space is limited in resolution, and expressive power and thus it does not necessarily provide the best support for simple inner product type of similarity measure [33], [46]. In kernel-based methods, in general, the original input data belonging to the data space $\mathcal{X}$ is mapped to a new space $\mathcal{H}$, known as the feature space [33]. In general, this mapping can be represented by a nonlinear mapping function φ_i, i.e.,

$$\varphi_i : \mathcal{X} \to \mathcal{H}, \qquad \mathbf{a} \to \varphi_i(\mathbf{g}), \qquad \mathbf{g} \to \varphi_i(\mathbf{g}) \tag{25}$$

where $\mathbf{a}$ and $\mathbf{g}$ are input vectors in $\mathcal{X}$ which are mapped into a potentially much higher-dimensional feature space $\mathcal{H}$. Then, a given similarity measure (i.e., the inner product) in the original space can be replaced with that of the feature space using the corresponding inner product $\langle \varphi_i(\mathbf{a}), \varphi_i(\mathbf{g})\rangle$. To this end, we build on the idea that the original space does not necessarily provide the best support for simple inner product type of similarity measure; thus the original data space is mapped into the feature space, aiming to obtain a richer space. Based on this idea, the unified detectors (22) and (24) can now be re-expressed as

$$|\langle \varphi_i(\mathbf{a}(\beta, \kappa)), \varphi_i(\mathbf{g}(\beta, \kappa))\rangle|^2 \underset{H_0}{\overset{H_1}{\gtrless}} \varsigma''_i, \tag{26}$$

$$\frac{|\langle \varphi^{(n)}_{7+\kappa}(\mathbf{a}(1, \kappa)), \varphi^{(n)}_{7+\kappa}(\mathbf{g}(1, \kappa))\rangle|^2}{1 + \langle \varphi^{(d)}_{7+\kappa}(\mathbf{g}(1, \kappa)), \varphi^{(d)}_{7+\kappa}(\mathbf{g}(1, \kappa))\rangle} \underset{H_0}{\overset{H_1}{\gtrless}} \varsigma''_{7+\kappa} \tag{27}$$

where ς''_i for $i = 1, \ldots, 8$ denote new detection thresholds to achieve a given false alarm rate. In (27), we consider two

different nonlinear mapping functions $\varphi_{7+\kappa}^{(n)}$ and $\varphi_{7+\kappa}^{(d)}$ in the numerator (n) and denominator (d), respectively.

It should be noted that computing the $\langle\varphi_i(\mathbf{a}), \varphi_i(\mathbf{g})\rangle$ would be impossible unless the feature mapping $\varphi_i(.)$ is explicit. In addition, implementing $\langle\varphi_i(\mathbf{a}), \varphi_i(\mathbf{g})\rangle)$ directly in the feature space is not necessarily straight-forward or computationally efficient due to the high dimensionality of vectors $\varphi_i(\mathbf{a})$ and $\varphi_i(\mathbf{g})$. For example, if φ_i is selected to be a polynomial of order d, then the length of the vectors $\varphi_i(\mathbf{a})$ and $\varphi_i(\mathbf{g})$ is equal to $\frac{(N+d-1)!}{d!(N-1)!}$, which is a large value if either N or d is large [33]. For the most common real-valued Gaussian kernel, the dimensionality of the associated feature space is infinite. Hence, the direct implementation of the proposed detectors in the feature space, such as (26) and (27), is normally impractical, mainly because of the high dimentionality associated with φ_i as well as the lack of the knowledge about φ_i. Fortunately, in the kernel method, this mapping function can be defined implicitly; rather, we need to define a function, often called a kernel, such that [46]

$$\mathcal{K}_i(\mathbf{a}, \mathbf{g}) = \langle\varphi_i(\mathbf{a}), \varphi_i(\mathbf{g})\rangle \tag{28}$$

Interestingly, it is seen that the kernel function computes the similarity using the kernel function $\mathcal{K}_i$ in the input space $\mathcal{X}$ instead of the feature space $\mathcal{H}$. In such cases, we do not require to know the explicit form of the feature map φ_i, but instead, it is implicitly defined through the corresponding kernel function. This technique is known as *kernelization* or a *kernel trick* in the kernel theory. A function that takes as its input vectors in the original space and returns the inner product of the vectors in the feature space is called a kernel function. Thus, using kernels, we never need the coordinates of the data in the feature space, because the detection algorithms only require the inner products between data in the feature space, which can be obtained by kernel function. To illustrate this, consider second-order real polynomial (SORP) kernel defined as $\mathcal{K}_i(\mathbf{a}, \mathbf{g}) = (\mathbf{a}^T\mathbf{g} + \delta_i)^{d_i}$ with $d_i = 2$, where we consider $\mathbf{a} = [a_1, a_2]^T$ and $\mathbf{g} = [g_1, g_2]^T$ as a simplified example. In this case, the SORP kernel can be expanded as

$$\begin{aligned}\mathcal{K}_i(\mathbf{a}, \mathbf{g}) &= (a_1g_1 + a_2g_2 + \delta_i)^2 \\ &= \langle\varphi_i(\mathbf{a}), \varphi_i(\mathbf{g})\rangle = \varphi_i(\mathbf{a})^T\varphi_i(\mathbf{g})\end{aligned} \tag{29}$$

where

$$\varphi_i(\mathbf{a}) = [a_1^2, a_2^2, \sqrt{2\delta_i}a_1, \sqrt{2\delta_i}a_2, \sqrt{2}a_1a_2, \delta_i]^T, \tag{30a}$$

$$\varphi_i(\mathbf{g}) = [g_1^2, g_2^2, \sqrt{2\delta_i}g_1, \sqrt{2\delta_i}g_2, \sqrt{2}g_1g_2, \delta_i]^T. \tag{30b}$$

Similarly, in the case of $\delta_i = 0$, we find that

$$\varphi_i(\mathbf{a}) = [a_1^2, a_2^2, \sqrt{2}a_1a_2]^T, \tag{31a}$$

$$\varphi_i(\mathbf{g}) = [g_1^2, g_2^2, \sqrt{2}g_1g_2]^T. \tag{31b}$$

As can be seen from (30) (or (31)), the two-dimensional input space via nonlinear mapping φ_i is mapped onto a six (or three)-dimensional feature space, aiming to obtain a richer space. To see this, a binary classification example is considered in Fig. 2, where a two-dimensional original space $\mathcal{X}$, represented by

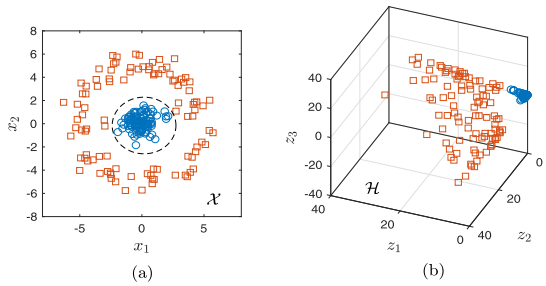

Fig. 2. A binary classification example, (a) data of two-dimensional input space $\mathcal{O}$, represented by $[x_1, x_2]$, (b) mapped data onto a three-dimensional feature space $\mathcal{F}$, represented by $\varphi_i(\mathbf{x}) = [z_1, z_2, z_3] = [x_1^2, x_2^2, \sqrt{2}x_1x_2]$, where data become linearly separable in the feature space $\mathcal{F}$.

$\mathbf{x} = [x_1, x_2]^T$, is mapped onto a three-dimensional feature space $\mathcal{H}$, represented by $\varphi_i(\mathbf{x}) = [z_1, z_2, z_3] = [x_1^2, x_2^2, \sqrt{2}x_1x_2]$. It is seen that the mapped data becomes linearly separable, i.e., the ellipse decision boundary of the input space of Fig. 2(a) becomes a hyperplane of Fig. 2(b) since ellipses can be written as linear equations in the entries of $[z_1, z_2, z_3]$ [33].

Remark 1: In general, there are different real-value kernel functions used in the literature, and the most common ones are the real polynomial $\mathcal{K}_i(\mathbf{x_1}, \mathbf{x_2}) = (\mathbf{x}_1^T\mathbf{x_2} + \delta_i)^{d_i}$ and the real Gaussian radial basis function (RBF) $\mathcal{K}_i(\mathbf{x_1}, \mathbf{x_2}) = \exp\left(-||\mathbf{x_1} - \mathbf{x_2}||^2/2\sigma_i^2\right)$, where the first belongs to the projective kernels and the latter is radial ones [33], [34]. Here, δ_i and d_i are respectively bias and order parameters of the polynomial kernel, while the single parameter $\sigma_i > 0$ is called the width of Gaussian RBF. Although the Gaussian RBF is the most popular, this radial kernel can deal with real-valued data sequences only. While the complex Gaussian RBF kernel with application in the complex kernel LMS algorithm has been introduced in [47], its applications to the target detection problems remain in obscurity especially when the Doppler frequency of interested target is assumed to be unknown [48]. In contrast, the polynomial kernel can also be used in complex domains. To do so, it is enough to end up with a complex inner product space. Based on this, for the first time, we use complex-valued polynomial kernel function for radar target detection problems, defined as $\mathcal{K}_i(\mathbf{x_1}, \mathbf{x_2}) = (\mathbf{x}_1^\dagger\mathbf{x_2} + \delta_i)^{d_i}$ with $d_i > 0$ [33]. This new complex-valued kernel can be served as a kernel function (in the sense of the kernel trick) if it satisfies two key properties: (1) positive semi-definiteness (i.e., $\mathcal{K}_i(\mathbf{x}_i, \mathbf{x}_i) \geq 0$ for $i = 1, 2$), and (2) symmetry (i.e., $\mathcal{K}_i(\mathbf{x}_1, \mathbf{x}_2) = \mathcal{K}_i^*(\mathbf{x}_2, \mathbf{x}_1)$). In our case, the positive semi-definiteness implies that $\mathcal{K}_i(\mathbf{x}_i, \mathbf{x}_i) = (\langle\mathbf{x}_i, \mathbf{x}_i\rangle + \delta_i)_i^d = (||\mathbf{x}_i||^2 + \delta_i)^{d_i} \geq 0$ for $i = 1, 2$, which holds true for $\delta_i \geq 0$. The symmetry property requires that $(\mathbf{x}_1^\dagger\mathbf{x_2} + \delta_i)^{d_i} = (\mathbf{x}_2^T\mathbf{x}_1^* + \delta_i^*)^{d_i}$, implying that δ_i must be a real value. All of these mean that $\mathcal{K}_i(\mathbf{x}_1, \mathbf{x}_2) = (\mathbf{x}_1^\dagger\mathbf{x}_2 + \delta_i)^{d_i}$ with $d_i > 0$ is a valid complex-valued kernel function provided that $\delta_i \geq 0$.

Remark 2: Let us consider (22) and (26), for example, and assume that each element of vectors $\mathbf{a}(\beta, \kappa)$, $\mathbf{g}(\beta, \kappa)$, $\varphi_i(\mathbf{a}(\beta, \kappa))$ and $\varphi_i(\mathbf{g}(\beta, \kappa))$ can be considered as feature in the original (input) or feature (transformed) spaces. In (22), the features are all the monomials of degree 1, while being monomials up to and including degree d_i when transforming the original data (i.e.,

$\mathbf{a}(\beta,\kappa)$ and $\mathbf{g}(\beta,\kappa)$) into the feature space (i.e., $\varphi_i(\mathbf{a}(\beta,\kappa))$ and $\varphi_i(\mathbf{g}(\beta,\kappa))$) equivalently through an appropriate polynomial kernel functions of order d_i. This can be seen from (29)–(30) for the special case of $d_i = 2$. Thus, it is shown that in the conventional detectors (22), only the inner product of all monomials with degree one is computed, while in the case of the kernelized detectors (26), the inner product of all monomials up to degree d_i are computed; allowing for richer feature space to be deployed in the detection.

B. Proposed Kernel-Based Detectors

The kernelization procedure consists of two basic steps. Firstly, we need to find an expression of the detector as a function of inner products between the original (input) data only. This representation is called the dual representation in contrast to the primal representation [46]. The second step consists of the substitution of the inner products by proper kernel functions, building on the kernel trick. As such, for the T-RaW(β,κ) detector, the kernel-based detector corresponding to (26) can be represented as

$$|\mathcal{K}_i\left(\mathbf{a}(\beta,\kappa),\mathbf{g}(\beta,\kappa);d_i,\delta_i\right)|^2 \underset{H_0}{\overset{H_1}{\gtrless}} \varsigma_i'' \tag{32}$$

where $i = 1,\ldots,6$. By comparing (22) and (32), it is observed that the inner products of $\langle \mathbf{a}(\beta,\kappa),\mathbf{g}(\beta,\kappa)\rangle$ is replaced with kernel function $\mathcal{K}_i(\mathbf{a}(\beta,\kappa),\mathbf{g}(\beta,\kappa);d_i,\delta_i)$. For the T-GLR$(\kappa)$ detector, the kernelized detector corresponding to (27) can be generally represented as

$$\frac{\left|\mathcal{K}_{7+\kappa}^{(n)}\left(\mathbf{a}(1,\kappa),\mathbf{g}(1,\kappa);d_{7+\kappa}^{(n)},\delta_{7+\kappa}^{(n)}\right)\right|^2}{1+\mathcal{K}_{7+\kappa}^{(d)}(\mathbf{g}(1,\kappa),\mathbf{g}(1,\kappa);d_{7+\kappa}^{(d)},\delta_{7+\kappa}^{(d)})} \underset{H_0}{\overset{H_1}{\gtrless}} \varsigma_{7+\kappa}'' \tag{33}$$

where, in general, kernel functions $\mathcal{K}_i$, $\mathcal{K}_i^{(n)}$ and $\mathcal{K}_i^{(d)}$ can be selected from different kernel functions. In our case with complex data, we adopt complex polynomial kernels and seek to tune their parameters to achieve maximum detection probability. By considering (32), the polynomial kernelized T-RaW(β,κ) detector can be expressed as

$$\left|\left(\langle \mathbf{a}(\beta,\kappa),\mathbf{g}(\beta,\kappa)\rangle+\delta_i\right)^{d_i}\right|^2 \underset{H_0}{\overset{H_1}{\gtrless}} \varsigma_i' \tag{34}$$

or, equivalently, as

$$|\langle \mathbf{a}(\beta,\kappa),\mathbf{g}(\beta,\kappa)\rangle+\delta_i|^2 \underset{H_0}{\overset{H_1}{\gtrless}} \varsigma_i \tag{35}$$

for $i = 1,\ldots,6$. The proposed detector (35) has the capability of flexibly tuning its selectivity (i.e., mismatch discrimination capability) or robustness (i.e., non-sensitive to mismatch) to the steering vector mismatch (SVM). This robustness or selectivity (RoS) capability is required for multifunction radar systems. For example, it is often desirable to reject the sidelobe targets (targets outside the antenna main beam) for tracking mode, while strong robustness of the system is desired for searching mode. To do so, we are able to change the tuning parameter, say β, to achieve desirable performance. For instance, the Rao-based test provides the best selectivity performance while the strongest robustness against steering vector mismatch is attained by the Wald-based detector. Among them, the TuRW-based detector provides a trade-off between the selectivity and robustness. In the following, this group of the proposed detectors is named kernelized and tunable RaW-based detectors, abbreviated as KT-RaW(β,κ).

For the general GLR-based detector (33), the corresponding polynomial kernel detectors can be given by

$$\frac{|(\langle \mathbf{a}(1,\kappa),\mathbf{g}(1,\kappa)\rangle+\delta_{7+\kappa}^{(n)})^{d_{7+\kappa}^{(n)}}|^2}{1+(\langle \mathbf{g}(1,\kappa),\mathbf{g}(1,\kappa)\rangle+\delta_{7+\kappa}^{(d)})^{d_{7+\kappa}^{(d)}}} \underset{H_0}{\overset{H_1}{\gtrless}} \varsigma_{7+\kappa} \tag{36}$$

In the context of the adaptive target detection in the C-MIMO radar, it is well-known that the GLR-based detectors provide the best detection performance in the matched cases. In our case, we aim to improve the above detection capability for the proposed polynomial kernel GLR-based detector by properly selecting the kernel parameters $d_{7+\kappa}^{(n)}$, $d_{7+\kappa}^{(d)}$, $\delta_{7+\kappa}^{(n)}$ and $\delta_{7+\kappa}^{(d)}$. This new group of the proposed detectors is also referred to as kernelized and tunable GLR-based detectors, abbreviated as KT-GLR(κ).

It is seen from (35) and (36) that the proposed detector depends on another tunable parameter κ to incorporate the prior distribution (PD) of the disturbance covariance matrix, if available, through the PD parameter, denoted by κ. Thus, the proposed detectors can be tuned based on the tuning RoS parameter to achieve robust or selective performance in the presence of SVM as well as to switch between the Bayesian or non-Bayesian based detectors through the PD parameter.

V. CFAR Property

In this section, we exploit the principle of invariance to examine the potential CFAR behavior of the proposed KT-RaW$(\beta,0)$ and KT-GLR(0) detectors against the nuisance parameter $\mathbf{R}$. It is known that the invariant test statistics (ITSs) can be expressed as some vector-valued functions of compressed data, namely the maximal invariance (MI). In addition, the distributions of ITSs can be parametrized by another low-dimensional function of parameter space, named the induced maximal invariance (IMI) [49]–[56]. Based on this strategy, we aim to achieve that the nuisance parameters are compacted in the IMI or removed from the considered problem, which could lead to CFAR tests. To proceed in this way, let us define two unitary matrices

$$\mathbf{U} = \left[\frac{\mathbf{b}}{||\mathbf{b}||},\mathbf{U}_2\right] \in C^{K\times K} \tag{37}$$

$$\mathbf{V} = \left[\frac{\mathbf{a}_R}{||\mathbf{a}_R||},\mathbf{V}_2\right] \in C^{N\times N} \tag{38}$$

such that $\mathbf{U}_2^\dagger\mathbf{b} = 0$ and $\mathbf{V}_2^\dagger\mathbf{a}_R = 0$. Now, it is straightforward to show that

$$\mathbf{Z} = \mathbf{V}^\dagger\mathbf{Y}\mathbf{U} = \begin{cases} H_0 : \mathbf{W} \\ H_1 : \alpha_1||\mathbf{a}_R||||\mathbf{b}||\mathbf{e}_1\mathbf{e}_1^T + \mathbf{W}. \end{cases} \tag{39}$$

It is seen that the above unitary matrices have been applied to $\mathbf{Y}$ to rotate the signal vectors $\mathbf{a}_R$ and $\mathbf{b}$ into the direction of the first standard vector $\mathbf{e}_1$. Here, $\mathbf{W}$ have IID columns distributed as circularly symmetric, complex Gaussian multivariate vectors with zero mean and unknown covariance matrix $\mathbf{V}^\dagger\mathbf{R}\mathbf{V}$, i.e., $\mathbf{w}_l \sim \mathcal{CN}(\mathbf{0}, \mathbf{V}^\dagger\mathbf{R}\mathbf{V})$ for $l = 1, \ldots, QK$.

This new problem is invariant under the group of transformations, $\mathcal{G}$, defined as

$$g(\mathbf{Z}) = \mathbf{F}\mathbf{Z}\mathbf{H} = \begin{bmatrix} \beta_1 & \beta_2^\dagger \\ \mathbf{0} & \mathbf{M} \end{bmatrix} \mathbf{Z} \begin{bmatrix} 1 & \mathbf{0}^T \\ \mathbf{0} & \mathbf{Q} \end{bmatrix} \tag{40}$$

where $g \in \mathcal{G}$ and $\beta_1 \neq 0$, $\beta_2 \in C^{(N-1)\times 1}$, $\mathbf{M} \in C^{(N-1)\times(N-1)}$ are arbitrary, and $\mathbf{Q} \in C^{(K-1)\times(K-1)}$ is a unitary matrix [49]. Here, we obtain

$$g(\mathbf{Z}) = \begin{cases} H_0 : \tilde{\mathbf{W}} \\ H_1 : \beta_1\alpha_1||\mathbf{a}_R||||\mathbf{b}||\mathbf{e}_1\mathbf{e}_1^T + \tilde{\mathbf{W}}. \end{cases} \tag{41}$$

where the columns of $\tilde{\mathbf{W}}$ have the same covariance matrix of $\mathbf{F}\mathbf{R}\mathbf{F}^\dagger$ instead of $\mathbf{V}^\dagger\mathbf{R}\mathbf{V}$. This means that the problem is invariant under the transformations (40) since the unknown parameter space changes form $\Theta = [\alpha_1, \mathbf{V}^\dagger\mathbf{R}\mathbf{V}]$ to new one as $\Theta = [\beta_1\alpha_1, \mathbf{F}\mathbf{R}\mathbf{F}^\dagger]$.

In our case, similar to [49], it is easy to show that the 2-dimensional maximal invariance to the group of transformations $\mathcal{G}$ can be obtained as

$$\begin{bmatrix} l_1 \\ l_2 \end{bmatrix} = \begin{bmatrix} \frac{|\mathbf{a}_R^\dagger \mathbf{R}_s^{-1}\mathbf{x}_b|^2}{\mathbf{a}_R^\dagger\mathbf{R}_s^{-1}\mathbf{a}_R} \\ \mathbf{x}_b^\dagger\mathbf{R}_s^{-1}\mathbf{x}_b \end{bmatrix} \tag{42}$$

where $\mathbf{R}_s = \mathbf{Y}\mathbf{D}^\perp\mathbf{Y}^\dagger$ and $\mathbf{x}_b = \mathbf{Y}\mathbf{b}$. The distribution of (42) has been obtained in [49] and shown that it depended only on a single IMI, playing the role of signal-to-noise ratio (SNR). Thus, under H_0 hypothesis, its distribution is independent of any parameters, resulting in CFAR behavior against the nuisance parameter $\mathbf{R}$. This means that we can obtain CFAR tests when exploiting test statistics that are a function of maximal invariances l_1 and l_2. These tests are known as invariant tests, where they are immune to the nuisance parameter $\mathbf{R}$ or they do not distinguish between scenarios differing in this nuisance parameter.

In our case, after some algebra manipulations, the unified T-RaW$(\beta, 0)$ and T-GLR(0) detectors can be written as a function of maximal invariances l_1 and l_2, represented by

$$\Lambda_{\text{T-RaW}}(\mathbf{Y}; \beta, 0) = \frac{l_1}{(1 + \beta l_2)(1 + \beta(l_2 - l_1))}, \tag{43}$$

$$\Lambda_{\text{T-GLR}}(\mathbf{Y}; 0) = \frac{l_1}{1 + l_2}. \tag{44}$$

Thus, we observe that the statistics of T-RaW$(\beta, 0)$ and T-GLR(0) detectors are both functions of maximal invariances, leading to nice CFAR invariant detectors with respect to the nuisance parameter $\mathbf{R}$[1]. As a result, the distribution of $\langle \mathbf{a}(\beta, 0), \mathbf{g}(\beta, 0)\rangle$ in the T-RaW$(\beta, 0)$ detector can be parameterized by the SNR only, leading to CFAR tests against the nuisance parameter $\mathbf{R}$ when working with statistic $|\langle \mathbf{a}(\beta, 0), \mathbf{g}(\beta, 0)\rangle + \delta_i|^2$ in the KT-RaW$(\beta, 0)$ detector for any value of δ_i. Similarly, for the KT-GLR(0) detector, we get CFAR detector when working with components $(\langle \mathbf{a}(1, 0), \mathbf{g}(1, 0)\rangle + \delta_7^{(n)})^{d_7^{(n)}}$ and $(\langle \mathbf{g}(1, \kappa), \mathbf{g}(1, \kappa)\rangle + \delta_7^{(d)})^{d_7^{(d)}} = (l_2 + \delta_7^{(d)})^{d_7^{(d)}}$. To get more insight, consider the special case of the KT-GLR(0) detector when $\delta_7^{(n)} = 0$, i.e.,

$$\frac{l_1^{d_7^{(n)}}}{1 + (l_2 + \delta_7^{(d)})^{d_7^{(d)}}} \underset{H_0}{\overset{H_1}{\gtrless}} \varsigma_7 \tag{45}$$

This reveals that the KT-GLR(0) detector possesses CFAR behavior for any value of $d_7^{(n)}$, $\delta_7^{(d)}$ and $d_7^{(d)}$ since it is a function of maximal invariants l_1 and l_2, namely we can set the detection threshold of KT-GLR(0) detector without knowing the actual nuisance parameter $\mathbf{R}$.

VI. Simulation Results

In this section, some simulation results are provided to examine and compare the detection performance of the four general T-RaW(β, κ) (including Rao, Wald, TuRW, BRao, BWald, BTuRW as special cases), T-GLR(κ) (including GLR and BGLR as special cases), KT-RaW(β, κ) (including KRao, KWald, KTuRW, KBRao, KBWald, KBTuRW as special cases) and KT-GLR(κ) (including KGLR and KBGLR as special cases) detectors [see Tables II and III for more specifications]. To do this, the number of transmit/receive antennas is set 10 (i.e., $N = M = 10$) and the desired false alarm probability of $p_{fa} = 10^{-3}$ is considered. The empirical false alarm and detection probability of the above detectors are determined by 10^5 Monte-Carlo (MC) simulation runs. Unless otherwise stated, we set tunable parameter β of KTuRW and KBTuRW equal to 0.5. In our simulation, we assume that each transmit antenna uses orthogonal Hadamard waveforms of length $Q = 16\mu$ with $\mu = 1, 2$ and unit power. Let us define the actual steering vector by $\mathbf{a}'_R$, while $\mathbf{a}_R$ is the nominal one used for detector design. To evaluate the detection performance, the signal-to-clutter ratio (SCR) of the general proposed classical detectors (i.e., T-RaW$(\beta, 0)$, T-GLR(0), KT-RaW$(\beta, 0)$ and KT-GLR(0)) is defined by

$$\text{SCR} = |\alpha_1|^2||\mathbf{R}^{-\frac{1}{2}}\mathbf{a}'_R||^2||\mathbf{b}||^2 \tag{46}$$

where it is

$$\text{SCR} = |\alpha_1|^2||\mathbf{R}_0^{-\frac{1}{2}}\mathbf{a}'_R||^2||\mathbf{b}||^2 \tag{47}$$

for the general proposed Bayesian detectors such as T-RaW$(\beta, 1)$, T-GLR(1), KT-RaW$(\beta, 1)$ and KT-GLR(1). The target's DOA is set equal to 10^0 and it is assumed that the $[\mathbf{R}]_{ij} = \sigma_c^2\rho^{|i-j|}$ ($[\mathbf{R}_0]_{ij} = \sigma_c^2\rho^{|i-j|}$), where ρ and σ_c^2 are respectively the one-lag correlation coefficient and clutter power. The proposed CFAR detectors are not sensitive to the values of ρ and σ_c^2; however, we set them equal to 0.9 and 1, respectively. In the case of the Bayesian-based detector, we set γ equal to 12.

[1]The CFAR behavior of these two detectors have been proven in [31] by obtaining the closed-form expressions for the false alarm probabilities.

TABLE III
PROPOSED TUNABLE ADAPTIVE DETECTORS BASED ON (35) AND (36), RESPECTIVELY NAMED KT-RAW(β,κ) AND KT-GLR(κ) IN GENERAL

Detector	Special Detectors	(β,κ)	Threshold	Polynomial Parameters
KT-RaW(β,κ)	KRao	$(1,0)$	ς_1	δ_1
	KWald	$(0,0)$	ς_2	δ_2
	KTuRW	$(\beta\geq 0,0)$	ς_3	δ_3
	KBRao	$(1,1)$	ς_4	δ_4
	KBWald	$(0,1)$	ς_5	δ_5
	KBTuRW	$(\beta\geq 0,1)$	ς_6	δ_6
KT-GLR(κ)	KGLR	$(1,0)$	ς_7	$d_7^{(n)}$, $\delta_7^{(n)}$, $d_7^{(d)}$, $\delta_7^{(d)}$
	KBGLR	$(1,1)$	ς_8	$d_8^{(n)}$, $\delta_8^{(n)}$, $d_8^{(d)}$, $\delta_8^{(d)}$

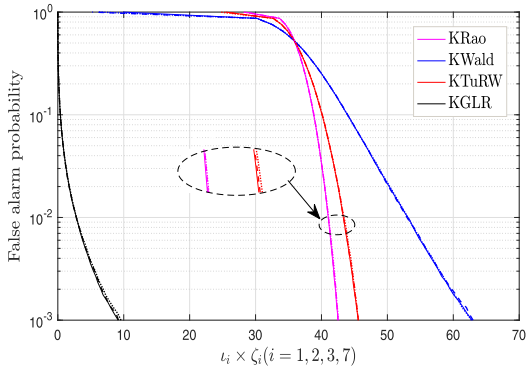

Fig. 3. Monte-Carlo false alarm probabilities as functions of detection thresholds ζ_1 (i.e., $\iota_1=1$), ζ_2 (i.e., $\iota_2=1$), ζ_3 (i.e., $\iota_3=1$) and ζ_4 (i.e., $\iota_4=2$) for the proposed KRao, KWald, KTuRW and KGLR detectors for different values of $\rho=0.3,0.6,0.9$ and when $Q=16$, indicating CFAR property against ρ. The lines denote the results of $\rho=0.9$, '- -' stands for $\rho=0.6$, and '... ' is for $\rho=0.3$. Here, the kernel parameters are set equal to $\delta_i=3$ for $i=1,\ldots,6$, $d_7^{(n)}=4$, $d_7^{(d)}=4$, $\delta_7^{(n)}=1.35$ and $\delta_7^{(d)}=5$.

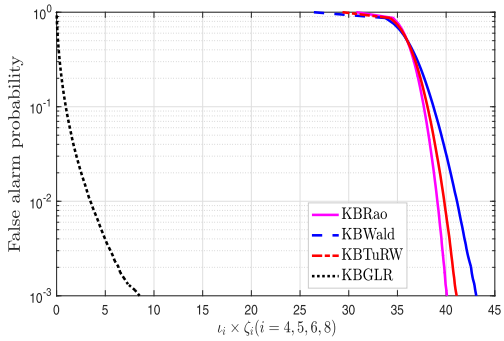

Fig. 4. Monte-Carlo false alarm probabilities as functions of detection thresholds ζ_1 (i.e., $\iota_1=1$), ζ_2 (i.e., $\iota_2=1$), ζ_3 (i.e., $\iota_3=1$) and ζ_4 (i.e., $\iota_4=10^{-3}$) for the proposed KBRao, KBWald, KBTuRW and KBGLR detectors. Here, the kernel parameters are set equal to $\delta_i=5$ for $i=1,\ldots,6$, $d_8^{(n)}=6$, $d_8^{(d)}=1$, $\delta_8^{(n)}=2.2$ and $\delta_8^{(d)}=4$.

In addition, in the following, we only consider the single pulse scenario, i.e., $K=1$.

A. False-Alarm Probability Versus Threshold

For the proposed KRao, KWald, KTuRW and KGLR detectors, the false alarm probabilities versus the detection threshold are evaluated and plotted in Fig. 3 for three different values of ρ and when $Q=16$. The detector thresholds are determined by 10^7 Monte-Carlo (MC) simulation runs to assure the reliability of the results.In Fig. 3, the lines denote the results of $\rho=0.9$, '- -' stands for $\rho=0.6$, and '...' is for $\rho=0.3$. From Fig. 3, it is seen that the above detectors have CFAR property against the correlation coefficient of the clutter covariance matrix. Thus, the obtained numerical results confirm our analytical CFAR conclusions obtained in Section V. The false alarm probabilities as a function of the detection threshold are depicted in Fig. 4 for the proposed KBRao, KBWald, KBTuRW and KBGLR detectors. Figs. 3 and 4 can be used to help us to set the decision thresholds of the proposed kernel-based detectors in the sequel for the desired false alarm of $p_{fa}=10^{-3}$.

B. Detection Performance Evaluations

For the proposed kernelized detectors, firstly, we need to select suitable parameters for the polynomial kernel as characterized in

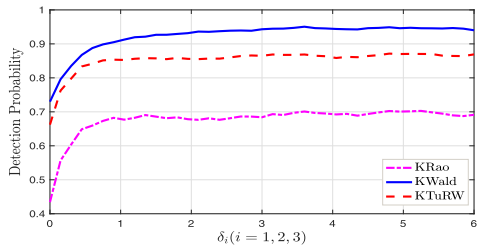

(a) Detector KT-RaW$(\beta,0)$

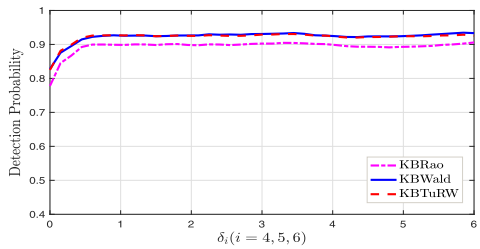

(b) Detector KT-RaW$(\beta,1)$

Fig. 5. Detection probability as a function of polynomial kernel's parameters of the proposed detector KT-RaW(β,κ) with $\kappa=0,1$ for $p_{fa}=10^{-3}$, $Q=16$ and when (a) SCR $=17$ dB and (b) SCR $=13$ dB.

Table III. In the detection theory framework, we are interested in tests that have maximum detection probability for a given false alarm probability. Next, based on these criteria, we are interested in finding the kernel parameters of the proposed detectors which maximize their detection probabilities. In Fig. 5, the detection

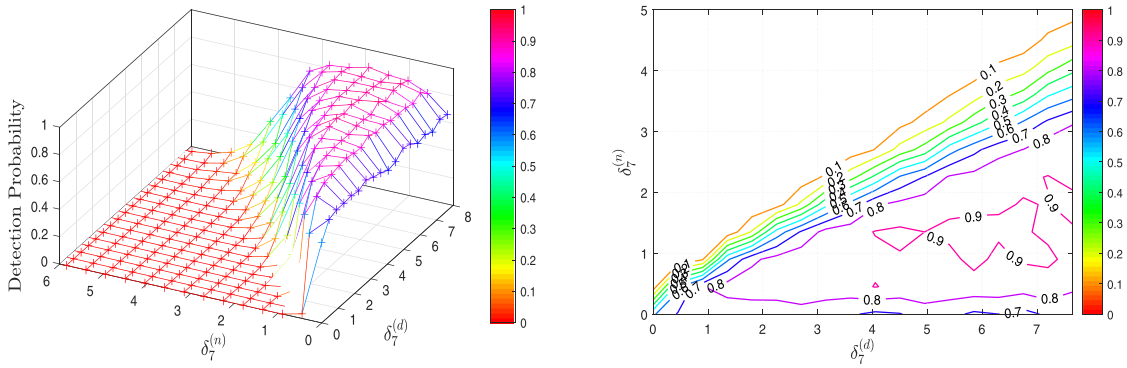

(a) Mesh plot (b) Contour plot

Fig. 6. Detection probability as a function of polynomial kernel's parameters $\delta_7^{(n)}$ and $\delta_7^{(d)}$ of the proposed detector KT-GLR(0) when $p_{fa} = 10^{-3}$, $Q = 16$, $d_7^{(n)} = 4$, $d_7^{(d)} = 4$ and SCR $= 16$ dB.

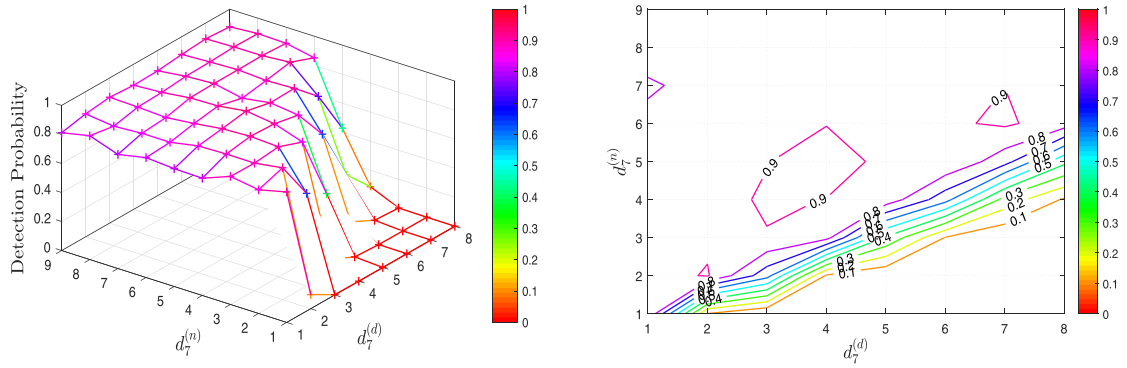

(a) Mesh plot (b) Contour plot

Fig. 7. Detection probability as a function of polynomial kernel's parameters $d_7^{(n)}$ and $d_7^{(d)}$ of the proposed detector KT-GLR(0) when $p_{fa} = 10^{-3}$, $Q = 16$, $\delta_7^{(n)} = 1.35$, $\delta_7^{(d)} = 5$ and SCR $= 16$ dB.

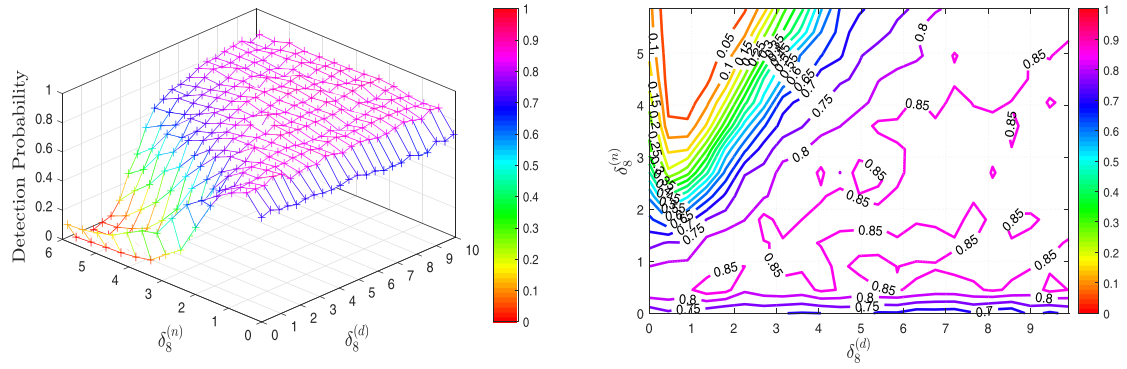

(a) Mesh plot (b) Contour plot

Fig. 8. Detection probability as a function of polynomial kernel's parameters $\delta_8^{(n)}$ and $\delta_8^{(d)}$ of the proposed detector KT-GLR(1) when $p_{fa} = 10^{-3}$, $Q = 16$, $d_8^{(n)} = 1$, $d_8^{(d)} = 6$ and SCR $= 12$ dB.

probability of the proposed KT-RaW(β, κ) detector as a function of δ_i is plotted when we set $p_{fa} = 10^{-3}$. Fig. 5(a) assumes SCR $= 17$ dB, while it is SCR $= 13$ dB in Fig. 5(b). In this case, it is observed that the value of $\delta_i \geq 3$ results in the best detection performance. In the following, we use these parameters to compare the detection performance of the proposed detectors with that of their counterparts. For the proposed KT-GLR(0) detector the above simulation is repeated and the results are shown in Fig. 6 for different values of parameters $\delta_7^{(n)}$ and $\delta_7^{(d)}$ and when $d_7^{(n)} = 4$ and $d_7^{(d)} = 4$. This figure clearly indicates that it is important to select proper values for $\delta_7^{(n)}$ and $\delta_7^{(d)}$ to maximize

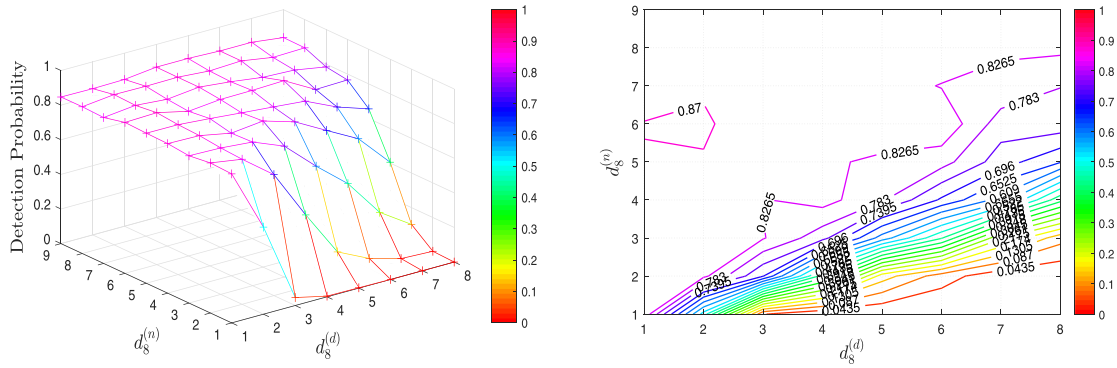

(a) Mesh plot (b) Contour plot

Fig. 9. Detection probability as a function of polynomial kernel's parameters $d_8^{(n)}$ and $d_8^{(d)}$ of the proposed detector KT-GLR(1) when $p_{fa} = 10^{-3}$, $Q = 16$, $\delta_8^{(n)} = 2.2$, $\delta_8^{(d)} = 4$ and SCR $= 12$ dB.

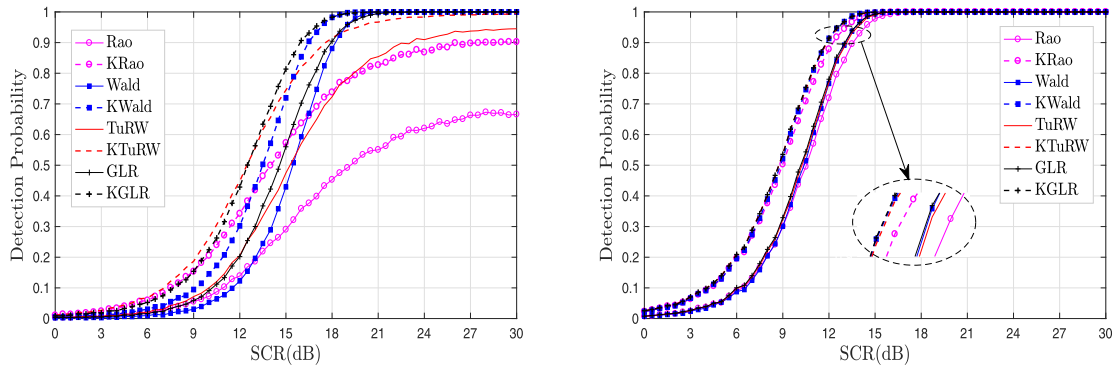

(a) Q=16 (b) Q=32

Fig. 10. Detection probability versus SCR in the matched spatial signal scenario for the unified detectors KT-RaW$(\beta, 0)$, KT-GLR(0), T-RaW$(\beta, 0)$ and T-GLR(0) when $M = N = 10$ and $p_{fa} = 10^{-3}$.

the detection probability. To see the effect of $d_7^{(n)}$ and $d_7^{(d)}$, which were set fixed in Fig. 6, we also plot in Fig. 7 the detection probability as functions of $d_7^{(n)}$ and $d_7^{(d)}$ when $\delta_7^{(n)} = 1.35$ and $\delta_7^{(d)} = 5$. It is observed from Fig. 7 that increasing $d_7^{(d)}$ will result in zero detection probability for the considered SCR. In the following investigation, we set $d_7^{(n)} = 4$, $d_7^{(d)} = 4$, $\delta_7^{(n)} = 1.35$ and $\delta_7^{(d)} = 5$ as suitable kernel parameters of the proposed KT-GLR(0) detector. For the proposed KT-GLR(1) detector, this examination is repeated and its results are shown in Figs. 8 and 9. The same trend, but with different kernel parameters, can be seen in comparison with that of the KT-GLR(0) detector. In this case, we obtain $d_8^{(n)} = 6$, $d_8^{(d)} = 1$, $\delta_8^{(n)} = 2.2$ and $\delta_8^{(d)} = 4$ as proper polynomial kernel parameters.

In Fig. 10, the detection performance of the proposed unified detectors KT-RaW$(\beta, 0)$ (KT-GLR(0)) and that of T-RaW$(\beta, 0)$ (T-GLR(0)) are compared together for different values of $Q = 16, 32$. It is seen that the proposed general detectors KT-RaW$(\beta, 0)$ have significantly better performances than that of their counterparts especially for small value of Q. In the case of $Q = 16$, the SCR gain improvements are about 11 dB, 2 dB, 3 dB and 2 dB, respectively, for the proposed KRao, KWald, KTuRW and KGLR at the detection probability of 0.68. In contrast, these improvements reduce to values of about 1.5 dB for $Q = 32$. For the proposed KT-RaW$(\beta, 1)$ (KT-GLR(1)) and that of T-RaW$(\beta, 1)$ (T-GLR(1)), these simulation results are repeated and the results are shown in Fig. 11. In this case, we obtain SCR gain improvement of about 1.5 dB and 1 dB for all the proposed Bayesian-based detectors for $Q = 16$ and $Q = 32$, respectively.

According to the Remark 2, the above improvements in the detection performance through the proposed kernel-based detectors are obtained due to exploiting the richer features of the transformed data (i.e., monomial features with degree up to d_i or $d_{7+\kappa}^{(n)}$) as compared to that of the original data represented by monomials with degree one. Thus, while the conventional detectors are efficient in finding linear relations, the kernel-based detectors provide generally a richer space to exploit both linear and nonlinear relations of the received data.

Up to this point, we have considered the matched spatial signal scenario. In the following, we assume that the actual input signal to the receive antennas over the k-th pulse is $\alpha_1 \mathbf{a}_R' \mathbf{a}_T^\dagger \mathbf{P}_k$ ($\mathbf{a}_R'$ is

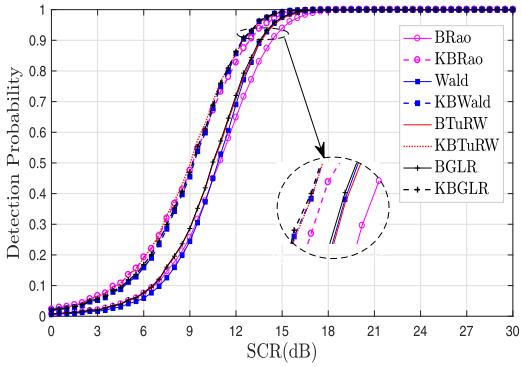

(a) Q=16

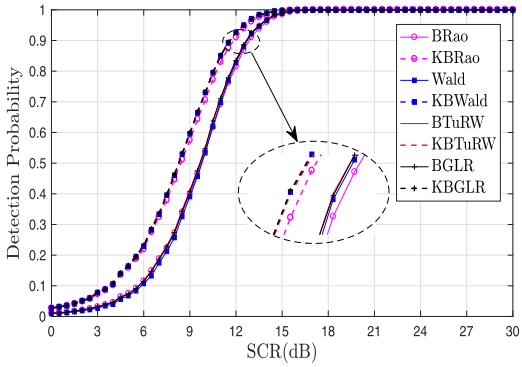

(b) Q=32

Fig. 11. Detection probability versus SCR in the matched spatial signal scenario for the unified detectors KT-RaW$(\beta,1)$, KT-GLR(1), T-RaW$(\beta,1)$ and T-GLR(1) when $M=N=10$ and $p_{fa}=10^{-3}$.

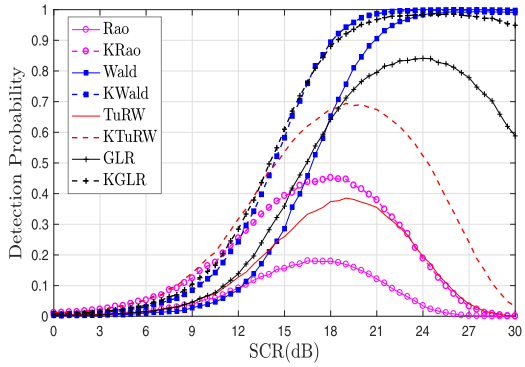

(a) $\kappa=0$

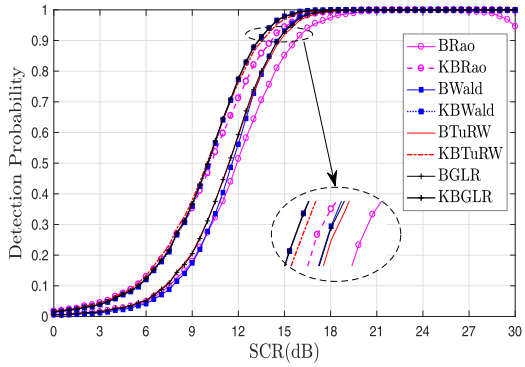

(b) $\kappa=1$

Fig. 12. Detection probability versus SCR in the mismatched spatial signal scenario for the unified detectors T-RaW(β,κ), T-GLR(κ), KT-RaW(β,κ), KT-GLR(κ) detectors with $\kappa=0,1$ when $M=N=10$, $Q=16$ and $p_{fa}=10^{-3}$.

called actual steering vector) but it is $\alpha_1\mathbf{a}_R\mathbf{a}_T^{\dagger}\mathbf{P}_k$ ($\mathbf{a}_R$ is called nominal steering vector) in used our signal model to derive the detectors. For the general proposed classical detectors (i.e., T-RaW$(\beta,0)$, T-GLR(0), KT-RaW$(\beta,0)$ and KT-GLR(0)), the squared sinusoid of the angle, say ϕ, between the whitened nominal steering vector and the whitened actual steering direction can be defined as

$$\sin^2(\phi)=1-\frac{|\mathbf{a}_R^{\dagger}\mathbf{R}^{-1}\mathbf{a}'_R|^2}{(\mathbf{a}_R^{\dagger}\mathbf{R}^{-1}\mathbf{a}_R)(\mathbf{a}_R'^{\dagger}\mathbf{R}^{-1}\mathbf{a}'_R)} \tag{48}$$

or, it is

$$\sin^2(\phi)=1-\frac{|\mathbf{a}_R^{\dagger}\mathbf{R}_0^{-1}\mathbf{a}'_R|^2}{(\mathbf{a}_R^{\dagger}\mathbf{R}_0^{-1}\mathbf{a}_R)(\mathbf{a}_R'^{\dagger}\mathbf{R}_0^{-1}\mathbf{a}'_R)} \tag{49}$$

for the general proposed Bayesian detectors such as T-RaW$(\beta,1)$, T-GLR(1), KT-RaW$(\beta,1)$ and KT-GLR(1).

In the first mismatched case, similar to [31], we assume that the actual DOA of the target of interest is 32^0, while it is considered equal to 30^0 for the nominal one. Fig. 12 shows the detection probability versus SCR for $Q=16$. In comparison to that of matched case, it is seen that the detection performance of all the considered detectors, especially the classical ones, are degraded as the SCR increases for the high SCR regime. In the proposed detector KT-RaW$(\beta,0)$, this degradation in detection performance becomes severe as the tunable parameter β increases due to more target signal contamination.

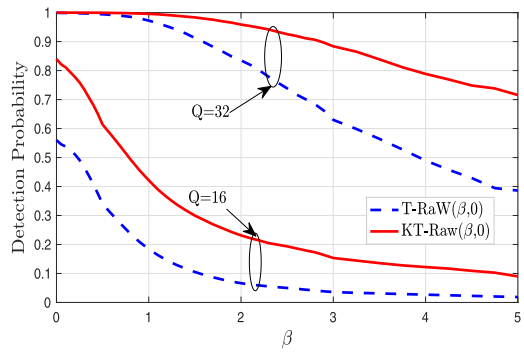

Fig. 13. Detection probability as a function of β for the unified detectors T-RaW$(\beta,0)$ and KT-RaW$(\beta,0)$ and when $M=N=10$, $Q=16,32$, SCR $=17$ dB and $p_{fa}=10^{-3}$.

From Fig. 12, it is observed that the detection performances of the KT-RaW$(\beta,1)$ detector is not degraded substantially for the SCR values in the range of $[0-27]$ dB due to exploiting the available prior knowledge of the covariance matrix. To examine this phenomenon for the proposed classical detectors, in Fig. 13, the detection probability as a function of β is depicted for the detectors of T-RaW$(\beta,0)$ and KT-RaW$(\beta,0)$, and when SCR $=17$ dB and $Q=16,32$. Using this figure, we can discuss the robustness and selectivity of the above detectors in the presence of a mismatched signal. This figure shows that by

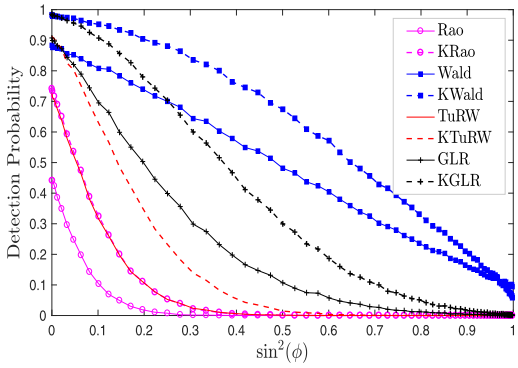

(a) Q=16 and SCR=18dB

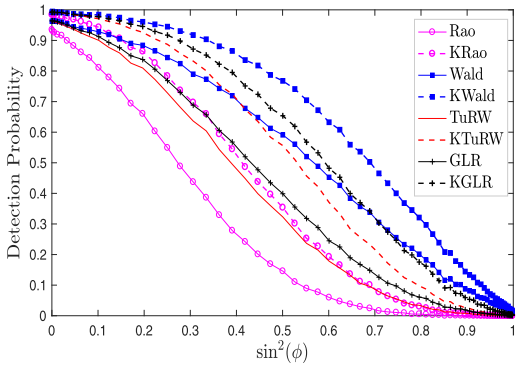

(b) Q=32 and SCR=15dB

Fig. 14. Detection probability as a function of $\sin^2(\phi)$ in the mismatched scenario for the unified detectors KT-RaW$(\beta, 0)$, KT-GLR(0), T-RaW$(\beta, 0)$ and T-GLR(0) when $M = N = 10$ and $p_{fa} = 10^{-3}$.

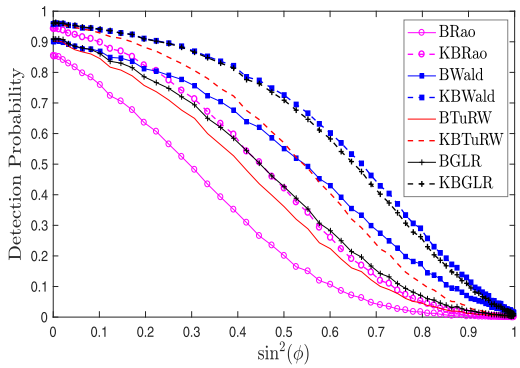

(a) Q=16 and SCR=14dB

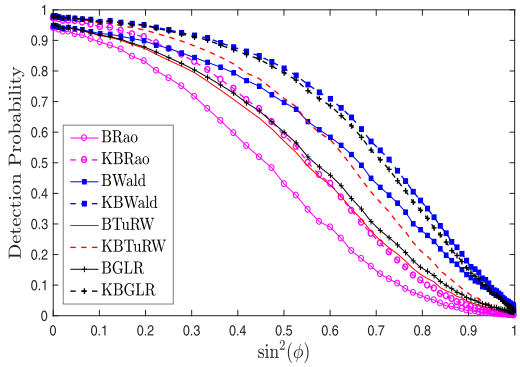

(b) Q=32 and SCR=14dB

Fig. 15. Detection probability as a function of $\sin^2(\phi)$ in the mismatched scenario for the unified detectors KT-RaW$(\beta, 1)$, KT-GLR(1), T-RaW$(\beta, 1)$ and T-GLR(1) when $M = N = 10$ and $p_{fa} = 10^{-3}$.

increasing the tunable parameter β the selectivity of the proposed detectors T-RaW$(\beta, 0)$ and KT-RaW$(\beta, 0)$ increases. As such, by increasing the tunable parameter β, the above-proposed detectors are less inclined to declare a detection if a mismatched signal is present, making them suitable for the tracking stage of a radar system. In contrast, more robustness is obtained by decreasing the tunable parameter β, which is suitable for the searching stage of a radar system. In the second examination of the mismatched signal, the detection performance as a function of $\sin^2(\phi)$ for the proposed detectors and their counterparts are depicted in Figs. 14 and 16. Fig. 14(a)–(b) assumes $Q = 16$ and SCR $= 18$ dB (SCR $= 15$ dB), while Fig. 16(a)–(b) corresponds to $Q = 32$ and SCR $= 14$ dB (SCR $= 14$ dB). In all cases, it is seen that the proposed KWald/KBWald detector offers the most robustness capability in the presence of mismatched signals, while the KRao/KBRao test has the best selectivity capability. From this figure, the significant detection performance improvement of the proposed kernelized detectors over their counterparts can be clearly seen.

From waveform design viewpoint, we are interested in designing a waveform resulting in a ambiguity function (or detector statistic output) with no sidelobe in range dimension. This characteristic makes it ideal for multi-target detection. To investigate this important aspect, we again consider the case of $Q = 16$ with $M = 10$ and use ten rows of the Hadamard matrix of order 16 as orthogonal waveforms (codes) transmitted over transmit

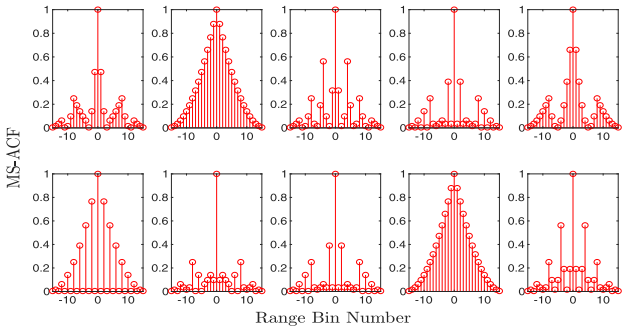

Fig. 16. Modulus-squared autocorrelation function (MS-ACF) of orthogonal Hadamard codes transmitted over different antennas as functions of range bin, where they result in the best ISL-based code in the output of the Rao statistic [see Fig. 17(a)].

antennas. To do this, the number of possible codes is equal to the number of combinations of Q items taken M at a time, which is equal to 8008 here. Through extensive search we choose the best integrated-sidelobe (ISL)-based code among the possible codes, where it is called Best code (Bcode) and represented in Table IV. Here, we assume a matched case in which the DOA of the target of interest is 32^0.

Modulus-squared autocorrelation functions (MS-ACFs) of different waveforms transmitted over transmit antennas as functions of range bins are shown in Fig. 16, where the Rao test

TABLE IV
BEST ISL-BASED TRANSMIT ANTENNA ORTHOGONAL HADAMARD WAVEFORMS OF LENGTH $Q = 16$ WHEN $M = 10$

Antenna number	Hadamard code
1	[1 -1 1 -1 -1 1 -1 1 -1 1 -1 1 1 -1 1 -1]
2	[1 -1 1 -1 1 -1 1 -1 1 -1 1 -1 1 -1 1 -1]
3	[1 -1 1 -1 -1 1 -1 1 1 -1 1 -1 -1 1 -1 1]
4	[1 1 -1 -1 1 1 -1 -1 -1 -1 1 1 -1 -1 1 1]
5	[1 1 1 1 1 1 1 1 -1 -1 -1 -1 -1 -1 -1 -1]
6	[1 1 -1 -1 1 1 -1 -1 1 1 -1 -1 1 1 -1 -1]
7	[1 1 -1 -1 -1 -1 1 1 -1 -1 1 1 1 1 -1 -1]
8	[1 -1 -1 1 1 -1 -1 1 -1 1 1 -1 -1 1 1 -1]
9	[1 1 1 1 1 1 1 1 1 1 1 1 1 1 1 1]
10	[1 1 -1 -1 -1 -1 1 1 1 1 -1 -1 -1 -1 1 1]

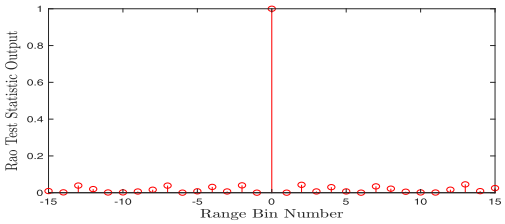

(a) Best ISL-Based code

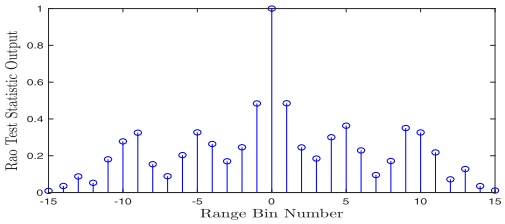

(b) Worst ISL-Based code

Fig. 17. Rao test statistic as functions of range bin for the obtained best and worst ISL-based codes.

statistic output,[2] is also depicted in Fig. 17(a). For comparison purposes, the worst ISL-based code, called Wcode, is also searched, where its Rao test statistic output is plotted in Fig. 17(b). We compare the detection performance of the considered detectors in three cases: 1) single-target scenario, 2) two-target scenario when the Bcode is chosen, 3) two-target scenario when the Wcode is used. For the multi-target scenario, two targets are considered with the same Doppler frequency but with the range bin differences of 12, and when the target under test has a SCR of 17 dB, while it is 14 dB for interfering target. The results of this simulation in terms of the Receiver Operating Characteristics (ROC) curves of all the detectors are plotted in Fig. 18. It can be observed that the presence of the interfering target can severely degrade the detection performances of the considered detectors when the Wcode is exploited, while it is better when the Bcode is chosen. This degradation in detection performance is due to the energy leakage of the strong interfering target into the adjacent range bins of the target under test. From Fig. 18, it can be observed that the proposed KGLR and KTuD detectors performs clearly better than the other detectors, being followed in performance by the proposed KWald and GLR detectors. In all cases, the Rao detector achieves the worst

[2]As shown in Fig. 18 the Rao detector achieves the worst performance.

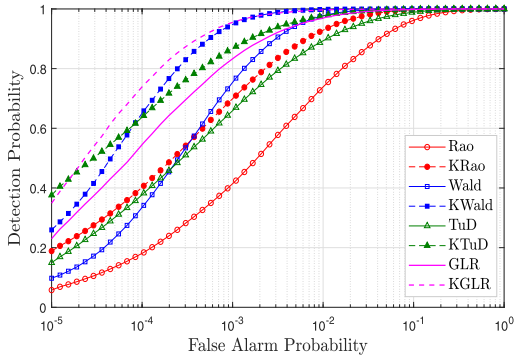

(a) Single-target detection,

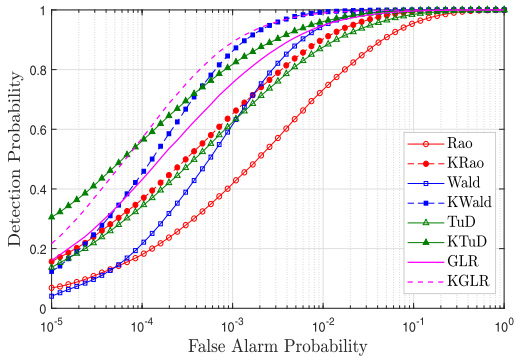

(b) Two-target detection by the Bcode,

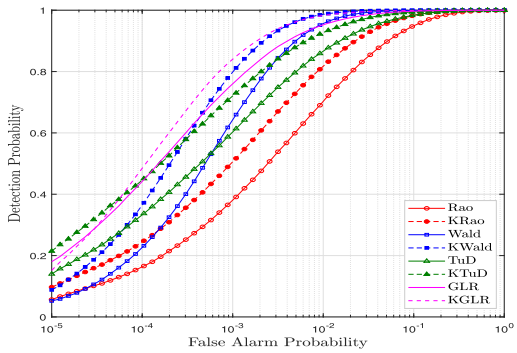

(c) Two-target detection by the Wcode.

Fig. 18. ROC curves of the proposed detectors and those of the previously proposed ones for $M = 10$, $Q = 16$, SCR $= 17$ dB for the target under test (TUT), SCR $= 14$ dB for the interfering target with a 12 range-bin separation with TUT.

performance. Additionally, by comparing Figs. 16 and 17, it can be seen that the resulting C-MIMO detector may have better range dimension characteristic as compared to the MS-ACF of different waveforms transmitted over transmit antennas. This highlights the importance of the waveform design problem in C-MIMO systems when the range dimension of the exploited detector is considered.

VII. CONCLUSION

We have adopted the theory of kernel to develop an exhaustive study for target detection in colocated MIMO radar. To do so, firstly, we have unified the detectors in the colocated

MIMO radar literatures. Then, they have been reformulated under the kernel method framework to improve their detection performances as measured by the SCR gains. To this end, we exploited the polynomial kernel functions and try to optimize the corresponding parameters of the functions to achieve a maximum detection probability under a fixed level of false alarm probability. Additionally, through the invariance theory, we investigated the potential CFAR behavior of the proposed classical detectors against the disturbance covariance matrix. Specifically, it was shown that all proposed classical detectors are robust against the disturbance covariance matrix. Finally, extensive simulation results are provided to indicate that the seven proposed detectors have better detection performance than their counterparts. In addition, the proposed detectors have tunable capability to select between the classical and Bayesian detectors as well as to choose between more selectivity or robustness against a mismatched signal, respectively, required for tracking or searching stages of a radar system. Finally, the importance of the waveform design for target detection in a multi-target scenario was investigated, where we showed that the proper choice of the signals transmitted via colocated MIMO antennas can improve the performance of adaptive colocated MIMO radar methods in multi-target scenarios.

Possible future extensions of our work might include the case of formulating an optimization problem to obtain optimal parameters of the complex-valued polynomial kernel. To do this, firstly, it is required to obtain closed-form expressions for the false alarm and detection probabilities of the kernelized detectors. Further extensions could be to devise a new kernel function through solving a complicated optimization problem.

ACKNOWLEDGMENT

The authors would like to acknowledge the Associate Editor and the anonymous reviewers who pointed out a number of suggested improvements.

REFERENCES

[1] S. M. Kay, *Fundamentals of Statistical Signal Processing*. Upper Saddle River, NJ, USA: Prentice-Hall, vol. 2, 1998.
[2] A. Zaimbashi, "Forward M-Ary hypothesis testing based detection approach for passive radar," *IEEE Trans. Signal Process.*, vol. 65, no. 10, pp. 2659–2671, Feb. 2017.
[3] E. J. Kelly, "An adaptive detection algorithm," *IEEE Trans. Aerosp. Electron. Syst.*, vol. AES-22, no. 1, pp. 115–127, Mar. 1986.
[4] E. Conte, M. Lops, and G. Ricci, "Asymptotically optimum radar detection in compound Gaussian clutter," *IEEE Trans. Aerosp. Electron. Syst.*, vol. AES-31, no. 2, pp. 617–625, Apr. 1995.
[5] A. Mehrabian and A. Zaimbashi, "Robust and blind eigenvalue-based multiantenna spectrum sensing under IQ imbalance," *IEEE Trans. Wireless Commun.*, vol. 17, no. 8, pp. 5581–5591, Jun. 2018.
[6] S. Kraut and L. L. Scharf, "The CFAR adaptive subspace detector is a scale-invariant GLRT," *IEEE Trans. Signal Process.*, vol. 47, no. 9, pp. 2538–2541, Sep. 1999.
[7] L. L. Scharf and B. Friedlander, "Matched subspace detectors," *IEEE Trans. Signal Process.*, vol. 42, no. 8, pp. 2146–2157, Aug. 1994.
[8] A. De Maio, "A new derivation of the adaptive matched filter," *IEEE Signal Process. Lett.*, vol. 11, no. 10, pp. 792–793, Oct. 2004.
[9] A. Zaimbashi, "Target detection in analogue terrestrial TV-based passive radar sensor: joint delay-doppler estimation," *IEEE Sensors J.*, vol. 17, no. 17, pp. 5569–5580, 2017.
[10] A. DeMaio, "Rao test for adaptive detection in Gaussian interference with unknown covariance matrix," *IEEE Trans. Signal Process.*, vol. 55, no. 7, pp. 3577–3584, Jul. 2007.
[11] A. M. Haimovich, R. S. Blum, and L. J. Cimini, "MIMO radar with widely separated antennas," *IEEE Signal Process. Mag.*, vol. 25, no. 1, pp. 116–129, Jan. 2008.
[12] A. Zaimbashi, M. R. Akhavan Saraf, and H. MirMohamad-Sadeghi, "Binary and fuzzy distributed CFAR detectors," in *Proc. Eur. Radar Conf., Amsterdam*, 2008, pp. 384–387.
[13] J. Li and P. Stoica, "MIMO radar with colocated antennas," *IEEE Signal Process. Mag.*, vol. 24, no. 5, pp. 106–114, Sep. 2007.
[14] A. Zaimbashi, "Broadband target detection algorithm in FM-based passive bistatic radar systems," *IET Radar, Sonar. Navigation*, vol. 10, no. 8, pp. 1485–1499, 2016.
[15] F. Bandiera, D. Orlando, and G. Ricci, "CFAR detection of extended and multiple point-like targets without assignment of secondary data," *IEEE Signal Process. Lett.*, vol. 13, no. 4, pp. 240–243, Apr. 2006.
[16] R. S. Raghavan, "Analysis of steering vector mismatch on adaptive noncoherent integration," *IEEE Trans. Aerosp. Electron. Syst.*, vol. 49, no. 4, pp. 2496–2508, Oct. 2013.
[17] A. Zaimbashi, "Multiband FM-based passive bistatic radar: target range resolution improvement," *IET Radar, Sonar Navigation*, vol. 10, no. 1, pp. 174–185, 2016.
[18] I. Bekkerman and J. Tabrikian, "Target detection and localization using MIMO radars and sonars," *IEEE Trans. Signal Process.*, vol. 54, no. 10, pp. 3873–3883, 2006.
[19] J. M. Anderson, "A generalized likelihood ratio test for detecting land mines using multispectral images," *IEEE Geosci. Remote Sens. Lett.*, vol. 5, no. 3, pp. 547–551, 2008.
[20] F. Bandiera, D. Orlando, and G. Ricci, "Advanced radar detection schemes under mismatched signal models," in *Synthesis Lectures on Signal Processing.*, San Rafael, CA, USA: Morgan and Claypool, 2009.
[21] F. Bandiera, D. Orlando, and G. Ricci, "A subspace-based adaptive sidelobe blanker," *IEEE Trans. Signal Process.*, vol. 56, no. 9, pp. 4141–4151, Sep. 2008.
[22] F. Bandiera, O. Besson, D. Orlando, and G. Ricci, "An improved adaptive sidelobe blanker," *IEEE Trans. Signal Process.*, vol. 56, no. 9, pp. 4152–4161, Sep. 2008.
[23] F. Bandiera, D. Orlando, and G. Ricci, "One- and two-stage tunable receivers," *IEEE Trans. Signal Process.*, vol. 57, no. 8, pp. 3264–3273, Aug. 2009.
[24] F. Bandiera, D. Orlando, and G. Ricci, "CFAR detection strategies for distributed targets under conic constraints," *IEEE Trans. Signal Process.*, vol. 57, no. 9, pp. 3305–3316, Sep. 2009.
[25] D. Orlando and G. Ricci, "A rao test with enhanced selectivity properties in homogeneous scenarios," *IEEE Trans. Signal Process.*, vol. 58, no. 10, pp. 5385–5390, Oct. 2010.
[26] J. Li and P. Stoica, *MIMO Radar Signal Processing*. Hoboken, NJ, USA: Wiley, 2009.
[27] J. Li and P. Stoica, "MIMO radar with colocated antennas," *IEEE Signal Process. Mag.*, vol. 24, no. 5, pp. 106–114, Sep. 2007.
[28] A. De Maio and M. Lops, "Design principles of MIMO radar detectors," *IEEE Trans. Aerosp. Electron. Syst.*, vol. 43, no. 3, pp. 886–898, Jul. 2007.
[29] L. Xu, J. Li, and P. Stoica, "Target detection and parameter estimation for MIMO radar systems," *IEEE Trans. Aerosp. Electron. Syst.*, vol. 44, no. 3, pp. 927–939, Jul. 2008.
[30] W. Liu, Y. Wang, J. Liu, and W. Xie, "Adaptive detection without training data in colocated MIMO radar," *IEEE Trans. Aerosp. Electron. Syst.*, vol. 51, no. 3, pp. 2469–2479, Jul. 2015.
[31] J. Liu, S. Zhou, W. Liu, J. Zheng, H. Liu, and J. Li, "Tunable adaptive detection in colocated MIMO radar," *IEEE Trans. Signal Process.*, vol. 66, no. 4, pp. 1080–1092, Feb. 2018.
[32] J. Liu, S. Zhou, W. Liu, J. Zheng, H. Liu, and J. Li, "Bayesian Detection for MIMO Radar in Gaussian Clutter," *IEEE Trans. Signal Process.*, vol. 66, no. 24, pp. 6549–6558, Dec. 2018.
[33] B. Scholkopf and A. J. Smola, *Learning With Kernels*. Cambridge, MA, USA: MIT Press, 2002.
[34] G. Ding, Q. Wu, Y. D. Yao, J. Wang, and Y. Chen, "Kernel-based learning for statistical signal processing in cognitive radio networks: Theoretical foundations, example applications, future directions," *IEEE Signal Process. Mag.*, vol. 30, no. 4, pp. 126–136, Jul. 2013.
[35] M. Mansouri, R. Baklouti, M. F. Harkat, M. Nounou, H. Nounou, and A. B. Hamida, "Kernel generalized likelihood ratio test for fault detection of biological systems," *IEEE Trans. Nanobioscience*, vol. 17, no. 4, pp. 498–506, Oct. 2018.

[36] H. Kwon and N. M. Nasrabadi, "Kernel matched subspace detectors for hyperspectral target detection," *IEEE Trans. Pattern Anal. Mach. Intell.*, vol. 28, no. 2, pp. 178–194, Feb. 2006.
[37] A. Margoosian, J. Abouei, and K. N. Plataniotis, "An accurate kernelized energy detection in Gaussian and non-gaussian/impulsive noises," *IEEE Trans. Signal Process.*, vol. 63, no. 21, pp. 5621–5636, Nov. 2015.
[38] L. Lily, S. Hou, and A. L. Anderso, "Kernelized generalized likelihood ratio test for spectrum sensing in cognitive radio," *IEEE Trans. Veh. Technol.*, vol. 67, no. 8, pp. 6761–6773, Aug. 2018.
[39] J. Liu, W. Liu, J. Han, B. Tang, Y. Zhao, and H. Yang, "Persymmetric GLRT Detection in MIMO Radar," *IEEE Trans. Veh. Technol.*, vol. 67, no. 12, pp. 11913–11923, Dec. 2018.
[40] H. Yang, Y. Wang, W. Xie, and Y. Di, "Persymmetric adaptive target detection without training data in collocated MIMO radar," in *Proc. CIE Int. Conf. Radar*, 2016, pp. 1–4.
[41] G. Foglia, C. Hao, G. Giunta, and D. Orlando, "Knowledge-aided adaptive detection in partially homogeneous clutter: Joint exploitation of persymmetry and symmetric spectrum," *Elsevier Digit. Signal Process.*, vol. 67, pp. 131–138, 2017.
[42] J. Liu, D. Orlando, P. Addabbo, and W. Liu, "SINR distribution for the persymmetric smi beamformer with steering vector mismatches," *IEEE Trans. Signal Process.*, vol. 67, no. 5, pp. 1382–1392, Mar. 2019.
[43] K. F. McDonald and R. S. Blum, "Exact performance of STAP algorithms with mismatched steering and clutter statistics," *IEEE Trans. Signal Process.*, vol. 48, no. 10, pp. 2750–2763, Oct. 2000.
[44] M. Rangaswamy, "Statistical analysis of the nonhomogeneity detector for non-Gaussian interference backgrounds," *IEEE Trans. Signal Process.*, vol. 53, no. 6, pp. 2101–2111, Jun. 2005.
[45] J. Liu, Z.-J. Zhang, Y. Yang, and H. Liu, "A CFAR adaptive subspace detector for first-order or second-order Gaussian signals based on a single observation," *IEEE Trans. Signal Process.*, vol. 59, no. 11, pp. 5126–5140, Nov. 2011.
[46] J. L. Rojo-lvarez, M. Martnez-Ramn, J. Muoz-Mar, and G. Camps-Valls, *Digital Signal Processing With Kernel Methods*. Hoboken, NJ, USA: Wiley, 2018.
[47] P. Bouboulis and S. Theodoridis, "The complex Gaussian kernel LMS algorithm," in *Proc. Int. Conf. Artif. Neural Netw.*, Sep. 2010, pp. 1–10.
[48] A. R. Salehi and A. Zaimbashi, "Radar target detection with kernel-based generalized likelihood ratio test," in *Proc. 6th Iranian Conf. Radar Surveillance Syst.*, Nov. 2019, pp. 1–5.
[49] S. Bose and A. O. Steinhardt, "A maximal invariant framework for adaptive detection with structured and unstructured covariance matrices," *IEEE Trans. Signal Process.*, vol. 43, no. 9, pp. 2164–2175, Sep. 1995.
[50] S. Bose and A. O. Steinhardt, "Optimum array detector for a week signal in unknown noise," *IEEE Trans. Aerosp. Electron. Syst.*, vol. 32, no. 3, pp. 911–922, Jul. 1996.
[51] T. S. Ferguson, *Mathematical Statistics Decision Theoretic Approach*. New York: Academic, 1967.
[52] E. L. Lehmann, *Testing Statistical Hypotheses*. 2nd ed. Belmont, CA, USA: Wadsworth, 1991.
[53] S. Kraut, L. L. Scharf, and R. W. Butler, "The adaptive coherence estimator: A uniformly most-powerful-invariant adaptive detection statistic," *IEEE Trans. Signal Process.*, vol. 53, no. 2, pp. 427–438, Feb. 2005.
[54] R. S. Raghavan, "Maximal invariants and performance of some invariant hypothesis tests for an adaptive detection problem," *IEEE Trans. Signal Process.*, vol. 61, no. 14, pp. 3607–3619, Jul. 2013.
[55] A. Zaimbashi, "Invariant subspace detector in distributed multiple-input multiple output radar: Geometry gain helps improving moving target detection," *IET Radar, Sonar Navigation*, vol. 10, no. 5, pp. 923–934, 2016.
[56] A. Ghobadzadeh, S. Gazor, M. Naderpour, and A. A. Tadaion, "Asymptotically optimal CFAR detectors," *IEEE Trans. Signal Process.*, vol. 64, no. 4, pp. 897–909, Feb. 2016.